

PHOTOCATALYTIC PROPERTIES OF ZINC OXIDE NANOSTRUCTURES
SYNTHESIZED USING SYNERGISTIC PULSE LASER ABLATION
AND HYDROTHERMAL METHODS

KHALDOON NAJI ABBAS AL-GBURI

A thesis submitted in fulfilment for the
requirements of the award of the degree of
Doctor of Philosophy (Physics)

Faculty of Science
Universiti Teknologi Malaysia

JULY 2017

Dedicated to my beloved family

To the most precious persons in my life, my parents, my wives, my brothers and sisters, and my sweetheart beautiful son and daughters.

ACKNOWLEDGEMENT

Thanks to ALLAH, the Most Gracious, the Most Merciful, the Most Bountiful who gave me the courage and patience to accomplish this research work. Without his help and mercy, this would not have come into reality.

I would like to deeply express my gratitude for the help and support from my Supervisor **Prof. Dr. Noriah Bidin** for their fascinating guidance, encouragement, patience and valuable comments throughout the research work. I was fortunate to be one of their graduate students. Their experience and creativity gave me great profit for carving my future career.

I would like to acknowledge the Universiti Teknologi Malaysia (UTM) for providing the facilities and support during this research. I wish also to thank Ministry of High Education of Iraq for their continuous help and support for this research.

Special thanks go to all those who have contributed directly and indirectly to the completion of this research and thesis. This includes UTM staff and my fellow postgraduate students who provided me with help and company during my study here.

Last, but not the least, my greatest thanks from my heart to my family for giving the unlimited supports and patience to complete my study. I would never ever forget their sacrifice that they have done for me. I appreciate the sacrifice of my parents, brothers and sisters in helping me morally to finish my study, god bless you all.

ABSTRACT

Mild growth conditions based novel techniques are essential for the controlled synthesis of zinc oxide (ZnO) nanostructure (ZNS) with desired properties. Most of the existing synthesis methods of ZNSs are limited by complicated growth conditions such as high vacuum, expensive devices, high temperature, long growth time and requirement of template. The freshwater pollution due to residual industrial organic dyes is presently being a major environmental concern that needs efficient photocatalytic materials to overcome it. To achieve these goals, this work synthesized good quality ZNS films using two different methods and evaluated the photodegradation of industrial methylene blue (MB) dye by these ZNS films under sunlight irradiation. Such films were grown on glass and silicon (Si) substrates via a simple hydrothermal method in the absence of any catalyst. Prepared samples were characterized using various techniques to determine their physical and optical properties. The effects of growth time and temperature, substrate type, nutrient pH and concentration on the morphology, size, crystallinity, and the emission properties of as-grown ZNS films were evaluated. Results showed that the morphology of these ZNSs was strongly influenced by the growth time, nutrient pH and concentration. A good quality ZNS was achieved within 5 min whereby nutrient solution with lower pH was appropriate for the growth of 1D ZNSs. However, higher pH values produced 3D flower-like ZNSs. Variation of growth temperature from 90-110 °C allowed good size-control of ZNSs. Growth conditions and substrate type dependent emission spectra were used to evaluate the optical band-gap energy. To get better control of the ZNS growth and evolving morphology, a novel catalyst-free and rapid preparation technique was adopted. In this method a mixture of precursor solution and ZnO nanoparticles (ZNPs) colloid/or only ZNPs colloid as a nutrient solution was used. Pulse laser ablation in liquid (PLAL) was combined with hydrothermal (H) method to develop PLAL-H growth technique. A Q-switched Nd:YAG laser with wavelength 532 nm, 8 ns pulse duration, and 10 Hz repetition rate was employed as the irradiation source. Metallic zinc target of 1 mm thick was used to produce colloidal ZNPs. The effects of varying growth time of 0.5, 5, 30 and 60 min and ablation energy of 200-400 mJ on the physical and optical properties of the grown ZNSs were examined. Four types of ZNSs with varying sizes and shapes were obtained on Si substrate at 110 °C for 5 min duration. Increasing ablation energy led to a substantial change of ZNS morphology and promoted the structure quality together with photoluminescence emission intensity. ZNSs synthesized under prolonged growth time of 60 min exhibited remarkable morphology alteration from rod/flower-like ZNSs to ZNPs with higher crystallinity and enlarged band-gap due to increase of nutrient pH of 10.5. Finally, the photocatalytic activities of the optimal ZNS films were assessed via sunlight driven photodegradation of MB dye. Experimental findings verified that the ZNPs prepared by PLAL-H technique possessed excellent photocatalytic efficiency (97.4%) towards degradation of MB dye. The observed boost in the photocatalytic activities was ascribed to the synergism of the improved surface area and band-gap modification. It was established that the proposed novel PLAL-H growth strategy is not only cost-effective but greatly useful for the rapid production of different quality of ZNSs at low temperature in a controlled way. This may overcome the shortcomings involving the effective exploitation of sunlight source towards practical photocatalytic applications of ZNSs.

ABSTRAK

Teknik novel berdasarkan keadaan pertumbuhan lambat adalah perlu untuk sintesis terkawal struktur-nano (ZNS) zink oksida (ZnO) dengan sifat yang dikehendaki. Kebanyakan kaedah sintesis ZNS sedia ada adalah terhad oleh keperluan pertumbuhan yang rumit seperti keadaan vakum tinggi, peralatan yang mahal, suhu tinggi, tempoh pertumbuhan yang lama dan keperluan terhadap templet. Pencemaran air tawar oleh sisa pewarna organik industri kini merupakan masalah persekitaran utama yang memerlukan bahan foto pemangkin yang efisien untuk mengatasinya. Untuk mencapai matlamat ini, kajian ini mensintesis filem ZNS yang berkualiti dengan menggunakan dua kaedah yang berbeza dan menilai fotodigredasi pewarna biru metalin (MB) industri oleh filem ZNS di bawah sinaran cahaya matahari. Filem tersebut dihasilkan di atas substrat kaca dan wafer silikon (Si) melalui kaedah hidroterma mudah tanpa pemangkin. Sampel yang disediakan dicirikan bagi menentukan ciri fizikal dan optik dengan menggunakan pelbagai teknik. Kesan masa pertumbuhan dan suhu, jenis substrat, pH dan kepekatan nutrien, terhadap morfologi, saiz, penghabluran, dan sifat pancaran filem ZNS telah dinilai. Hasil kajian menunjukkan bahawa morfologi ZNS ini sangat dipengaruhi oleh masa pertumbuhan, pH dan kepekatan nutrien. Kualiti ZNS yang baik telah dicapai dalam masa 5 minit apabila cecair nutrien dengan pH lebih rendah adalah sesuai untuk pertumbuhan ZNS 1D. Walau bagaimanapun, nilai pH yang lebih tinggi menghasilkan ZNS berbentuk bunga 3D. Perubahan suhu pertumbuhan dalam lingkungan 90-110 °C membolehkan kawalan saiz ZNS yang baik. Spektrum pancaran yang bergantung kepada keadaan pertumbuhan dan jenis substrat telah digunakan untuk menilai jurang tenaga optik. Untuk mencapai kawalan yang lebih baik ke atas pertumbuhan ZNS dan perkembangan morfologi, teknik penyediaan yang novel dan bebas pemangkin serta pantas telah digunakan. Dalam kaedah ini, campuran cecair pelopor dan koloid nanopartikel ZnO (ZNP)/atau hanya koloid ZNP telah digunakan sebagai cecair nutrien. Ablasi laser denyut dalam cecair (PLAL) telah digabungkan dengan kaedah hidroterma (H) untuk menghasilkan teknik pertumbuhan PLAL-H. Laser Nd:YAG pensuisan-Q dengan panjang gelombang 532 nm, tempoh denyutan 8 ns, dan kadar ulangan 10 Hz telah digunakan sebagai sumber sinaran. Sasaran logam zink dengan ketebalan 1 mm digunakan untuk menghasilkan koloid ZNP. Kesan masa pertumbuhan yang berbeza-beza dari 0.5, 5, 30 dan 60 minit dan tenaga ablati 200-400 mJ terhadap ciri fizikal dan optik ZNS telah diperiksa. Empat jenis ZNS dengan pelbagai saiz dan bentuk telah diperolehi pada substrat Si pada suhu 110 °C untuk tempoh 5 minit. Peningkatan tenaga ablati membawa kepada perubahan ketara pada morfologi ZNS dan mempromosikan kualiti struktur bersama-sama dengan keamatan pancaran kefotopendarcahayaan. ZNS yang disintesis di bawah masa pertumbuhan selama 60 minit mempamerkan transformasi morfologi luar biasa dari ZNS berbentuk rod/bunga ke ZNP dengan penghabluran yang lebih tinggi dan nilai jurang yang lebih besar disebabkan oleh peningkatan pH nutrien kepada 10.5. Akhir sekali, aktiviti fotopemangkin filem ZNS optimum telah dinilai terhadap fotodigredasi pewarna biru metalin (MB) berpacuan cahaya matahari. Hasil eksperimen mengesahkan bahawa ZNP yang disediakan oleh teknik PLAL-H memiliki kecekapan fotopemangkin yang sangat baik (97.4%) ke arah degradasi pewarna MB. Peningkatan yang diperhatikan dalam aktiviti fotopemangkin telah disifatkan sebagai sinergi peningkatan kawasan permukaan dan perubahan jurang jalur. Ternyata bahawa strategi pertumbuhan PLPAL-H novel yang dicadangkan ini bukan sahaja menjimatkan kos tetapi berguna untuk pengeluaran pantas secara terkawal ZNS dengan kualiti yang berbeza pada suhu rendah. Ini boleh mengatasi kelemahan yang melibatkan keberkesanan penggunaan sumber cahaya matahari untuk aplikasi praktikal fotopemangkin ZNS.

TABLE OF CONTENTS

CHAPTER	TITLE	PAGE
	DECLARATION	ii
	DEDICATION	iii
	ACKNOWLEDGEMENT	iv
	ABSTRACT	v
	ABSTRAK	vi
	TABLE OF CONTENTS	vii
	LIST OF TABLES	xiii
	LIST OF FIGURES	xv
	LIST OF ABBREVIATIONS	xxviii
	LIST OF SYMBOLS	xxxi
	LIST OF APPENDICES	xxxiv
1	INTRODUCTION	1
	1.1 Overview	1
	1.2 Photocatalytic Application	5
	1.3 Problem Statement	6
	1.4 Research Objectives	8
	1.5 Scope of Study	8
	1.6 Significance of Study	10
	1.7 Thesis Organization	10
2	LITERATURE REVIEW	12
	2.1 Introduction	12
	2.2 Properties ZnO Semiconductor	13

2.2.1	Crystal Structures	13
2.2.2	Optical Properties of ZnO	14
2.2.3	Electrical Properties of ZnO	16
2.3	Native Point Defects of ZnO Structure	18
2.4	Growth of ZnO Nanostructure	20
2.4.1	Pulse Laser Ablation in Liquid Method	21
2.4.1.1	Growth Mechanism and Experimental Setup of PLAL Method	23
2.4.1.2	Thermal Evaporation Mechanism	24
2.4.1.3	Growth Conditions of PLAL Method	27
2.4.2	Hydrothermal Growth Method	32
2.5	Controlled Mode of ZnO Nanostructure	38
2.5.1	Effects of Nutrient Concentration and Type on ZnO Nanostructures Properties	41
2.5.2	Influence of Growth Temperature and Time on ZnO Nanostructures Properties	42
2.5.3	Influence of Nutrient pH on ZnO Nanostructures Properties	44
2.5.4	Influence of Seed Layer on ZnO Nanostructures Properties	45
2.6	ZnO Nanostructures Thin Film Deposition	46
2.7	Application of ZnO Nanostructure Films for Photocatalysis	47
2.7.1	ZnO Nanostructures for Photocatalysis	49
2.7.2	Photocatalytic Mechanism of ZnO Nanostructures	50
2.7.2.1	Charge Carrier Generation	50
2.7.2.2	Charge Carrier Trapping	51
2.7.2.3	Charge Carrier Recombination	53
2.7.2.4	Photocatalytic Degradation of Dye Pollutants	53
2.7.3	Strategies for Improving Photocatalytic Efficiency of ZnO Nanostructures	55

	2.7.3.1	Band-Gap Modification of ZnO	55
	2.7.3.2	Photosensitization Process of ZnO Surface	56
	2.7.3.3	Architecture Adjustment of ZnO	56
	2.7.3.4	Optimization of ZnO Surface Area	57
	2.7.4	Methylene Blue as Organic Dye Pollutant	57
3	RESEARCH METHODOLOGY		60
	3.1	Introduction	60
	3.2	Methods for ZnO Nanostructures Synthesis	61
	3.2.1	Raw Materials	61
	3.2.2	Substrate Cleaning for ZnO Nanostructures Film Deposition	62
	3.2.3	Hydrothermal Method for ZnO Nanostructure Growth	62
	3.2.4	PLAL-H Technique for ZnO Nanostructures Growth	65
	3.2.4.1	Q-switched Nd:YAG Laser for Ablation of Zn Target	66
	3.2.4.2	PLAL Method for Colloidal ZnO Nanoparticles Synthesis	69
	3.2.4.3	PLAL-H Technique (Strategy I) for ZnO Nanostructure Films Deposition	72
	3.2.4.4	PLAL-H Technique (Strategy II) for ZnO Nanostructure Films Deposition	75
	3.3	Characterization Techniques	77
	3.3.1	Scanning Electron Microscope Imaging	77
	3.3.2	Energy Dispersive X-ray Spectrometer	78
	3.3.3	Transmission Electron Microscope Imaging	78
	3.3.4	X- Ray Diffraction Measurement	79
	3.3.5	Fourier Transform Infrared Spectrometer	82
	3.3.6	Photoluminescence Spectrometer	83

3.3.7	UV-Vis-NIR Spectrophotometer	84
3.4	Photocatalytic Activity Evaluation of ZNSs-based Films	84
4	RESULTS AND DISCUSSION	86
4.1	Introduction	86
4.2	Properties of ZnO Nanostructures Film Grown by Hydrothermal Method	87
4.2.1	Effects of Growth Time and Substrate on Nanostructures	88
4.2.1.1	Morphology, Size and Stoichiometric Ratio of Nanostructures	88
4.2.1.2	XRD Analysis of ZnO Nanostructure Film	94
4.2.1.3	Optical Properties of ZnO Nanostructure Films	97
4.2.2	Effect of Nutrient Solution ZnO Nanostructure Properties	100
4.2.2.1	Morphology Analysis	100
4.2.2.2	Structural Properties	102
4.2.2.3	FTIR Analysis of ZnO Nanostructure Films	103
4.2.2.4	Photoluminescence Properties	104
4.2.3	Effect of Nutrient pH on ZnO Nanostructure Films	105
4.2.3.1	Morphology Analysis	105
4.2.3.2	Structural Analysis	107
4.2.3.3	Photoluminescence Properties of ZnO Nanostructure Films	108
4.2.3.4	FTIR Spectra of ZnO Nanostructures Film	109
4.2.4	Influence of Growth Temperature on ZnO Nanostructure Films	110
4.2.4.1	Morphology Analysis	110

4.2.5	Growth Mechanism of ZnO Nanostructures	111
4.3	ZnO Nanostructures Synthesis via PLAL-H Method	115
4.3.1	Characterization of ZnO Nanoparticles Prepared via PLAL Method	116
4.3.1.1	Morphological Properties	116
4.3.1.2	Absorption Spectra of Colloidal ZnO Nanoparticles	120
4.3.2	Synthesis ZnO Nanostructure Films by PLAL-H Technique	121
4.3.2.1	Morphology Analysis of As-Grown ZnO Nanostructure Films	123
4.3.2.2	Structural Properties of ZnO Nanostructures	130
4.3.2.3	FTIR Analysis of ZnO Nanostructures	132
4.3.2.4	Absorption and Luminescence Properties of ZnO Nanostructures	133
4.3.2.5	Growth Mechanism of ZnO Nanostructures Obtained via PLAL-H Method	138
4.3.3	Influence of Laser Ablation Energy on the ZnO Nanostructures	142
4.3.3.1	Morphology Analysis of ZnO Nanostructures	142
4.3.3.2	Structural Analysis of ZnO Nanostructure Films	144
4.3.3.3	FTIR Analysis	145
4.3.3.4	Photoluminescence Properties of ZnO Nanostructures	146
4.4	Influence of PLAL-H Growth Conditions on ZnO Nanostructure Films	148
4.4.1	Morphology Analysis of As-Grown ZnO Nanostructures	149

4.4.2	Structural Properties of As-Grown ZnO Nanostructures	153
4.4.3	FTIR Analysis	154
4.4.4	Absorption and Photoluminescence Properties of As-Grown Samples	155
4.4.5	Growth Mechanism of As-Grown ZnO Nanostructures	159
4.5	Photocatalytic Applications of As-Grown ZnO Nanostructures	163
4.5.1	Photocatalytic Activity of As-Synthesized ZnO Nanostructure Films	163
4.6	Synergism in PLAL and Hydrothermal Methods	177
5	CONCLUSION AND RECOMMENDATIONS	179
5.1	Conclusions	179
5.2	Recommendations for Future Work	183
	REFERENCES	185
	Appendix A	207-208

LIST OF TABLES

TABLE NO.	TITLE	PAGE
2.1	Basic characteristics of stable wurtzite ZnO structure	1
2.2	Early literature review of synthesis ZNPs by pulse laser ablation method	28
2.3	Different reaction based solution for achieving diverse ZNSs using hydrothermal method	39
3.1	Growth parameters of hydrothermal method and achieved morphologies	63
3.2	Specification of Q-switched Nd:YAG laser (BKF-K9 model)	68
3.3	Growth parameters and conditions of PLAL-H technique	74
4.1	Growth parameters of hydrothermal method and morphology of achieved samples	87
4.2	Values of lattice constants, crystallite size, and micro-strain of ZMNSs deposited on glass and Si substrates for 3 hr duration	97
4.3	Growth conditions of PLAL-H technique (first strategy) and achieved samples	122
4.4	Growth conditions of PLAL-H technique (second strategy) and morphology of grown samples	149
4.5	Wavelength (λ , nm) and energy band-gap (E_g , eV) of PL emission peaks obtained for ZNSs at different nutrient pH values	156

4.6	Optimum photocatalytic ZNSs films grown by PLAL-H and hydrothermal methods	164
4.7	Display of photocatalytic efficiency of decolorization of MB suspension under various irradiation sources for various nanomaterials prepared via different growth techniques	174

LIST OF FIGURES

FIGURE NO.	TITLE	PAGE
1.1	Overview of different structures and geometries at nanoscale	2
1.2	SEM images of various ZNSs synthesized on Si substrates using hydrothermal method: (a, b and c) rod-like, (d) star-like, and (e and f) flower-like	3
1.3	Pictures showing the freshwater pollution (a and b) due to chemicals fallout and (c and d) its influence on the living organism	5
2.1	Crystal structure of ZnO: (a and b) hexagonal wurtzite structure unit and (c) cubic zinc-blende unit	14
2.2	Room temperature PL spectra of ZNWs with average diameters of 12 nm, 16 nm and 31 nm revealing a prominent UV peak at 380 nm and a broad visible peak	16
2.3	Energy level diagram for native defects in ZnO with defect ionization energies in the range of 1.6-3.01 eV	19
2.4	(a) Experimental setup for PLAL of solid target and (b) ablation process of the target material	24
2.5	Schematic illustration of the evolution of the laser-induced plasma in liquid leading to the growth of nano/microstructure: (a) generation of Zn plasma	

	having high temperature and pressure on the top of the Zn target immediately after single pulse irradiation, (b-c) adiabatic and ultrasonic expansion of the plasma and creation of Zn clusters, and (d) creation of ZNSs	26
2.6	Schematic diagram displays the formation process of different ZNSs dependent various laser fluence	31
2.7	TEM images of ZNSs prepared by PLAL at different increasing laser ablation energy: (a, b and c) ZnO morphology is varied from nanoflakes at 20 mJ to (d) ZNPs at 70 mJ, and to (e and f) short ZNRs at 120 mJ	32
2.8	Schematic representation of hydrothermal process: (a) experimental setup and (b) growth mechanism	34
2.9	FESEM images of different ZNSs morphology grown by hydrothermal method at 140 °C for 10 hr: (a) sphere, (b) rod, (c) sheet, and (d) wire	35
2.10	Schematic illustration of the growth mechanism steps using hydrothermal treatment under 80 °C for 12 hr: (A) primary growth units, (B) ZnO nuclei, (C) ZnO crystallites, and (D) flower-like ZNSs	37
2.11	Nutrient solution concentration dependent average diameters and lengths of the ZNWs synthesized via hydrothermal method	42
2.12	The growth time dependent (1-11 hr) UV-Vis absorption spectra of ZnO structures prepared by hydrothermal method	44
2.13	Schematic illustration the photogeneration of oxidizing species in ZnO photocatalysis and photocatalysis process by ZnO semiconductor	51
2.14	Schematic diagram revealing the molecular structure of the MB dye	58

3.1	Schematic presentation of hydrothermal method: (a) Oven, (b) autoclave glass (140 °C of volume 250 mL), (c) grown diverse ZNSs films with various morphology such as (d) flower-like, (e) rice-like, and (f) enclosed tube-like	63
3.2	The flowchart displaying the methodology ZNSs-based films preparation by hydrothermal method, various characterizations and their photocatalytic application toward MB dye photodegradation	64
3.3	Schematic diagram of: (a) pulsed Nd:YAG laser structure and (b) energy-level diagram for lasing action in Nd ³⁺ ion	67
3.4	Calibration of Q-switched Nd:YAG laser pulse energy at 532 nm, 8 ns and 10 Hz in range of 40-800 mJ/pulse	68
3.5	Depiction of PLAL method: (a) Photograph of PLAL system experimental setup with Zn-target under water, (b) schematic diagram of PLAL method for colloidal ZNPs synthesis, (c) actual ablation process and (d) the schematic diagrams of the ablation process	70
3.6	Photograph showing the achieved laser ablated products from Zn target immersed inside water	71
3.7	Flowchart displaying PLAL method based synthesis of colloidal suspension of ZNPs and their subsequent characterizations	72
3.8	Schematic presentation for the synthesis of ZNSs-based film by PLAL-H technique (First stage): (a) colloidal solution ZNPs preparation by PLAL method (denoted as N2), and (b) preparation of nutrient solution by mixing N1 and N2 subjected to hydrothermal treatment	73

3.9	The flowchart showing the growth of ZNSs-based films by PLAL-H technique using ZNPs colloid as nutrient solution, samples characterizations, and photocatalytic application	76
3.10	(a) Schematic presentation demonstrating the XRD from regular lattice planes following the Bragg's law, and (b) constructive and destructive interference patterns	80
3.11	Schematic diagrams showing the experimental setup to evaluate the photocatalytic activity of ZNSs films via the degradation of MB driven by solar radiation	85
4.1	FESEM images of ZNSs (samples L1, L2, L3 and L4) at different magnification grown for (A-a) 1 hr, (B-b) 2 hr, (C-c) 3 hr, and (D-d) 4 hr on glass (left column) and Si (right column) substrates. Inset in (c) is the tip of NR and red circle in (d) destroyed NRs	89
4.2	Growth time duration dependent average length and diameter of ZNRs synthesized on glass substrate	90
4.3	Distribution (length and diameter) of ZNRs (fitted to Gaussian) grown on glass substrate for the duration of (a-a1) 1 hr, (b-b1) 2 hr, (c-c1) 3 hr, and (d-d1) 4 hr. Similar behaviour was observed for samples grown on Si substrate	91
4.4	ZMNSs (samples L5 and L6) grown on glass substrate for 6 or 8 hr duration (a) FESEM images and (b) XRD pattern	92
4.5	EDX spectra of ZMNSs grown on glass substrate for 6 or 8 hr duration	93
4.6	EDX spectra of dense ZMNSs grown for 3 hr on: (a) glass and (b) Si substrates	94

- 4.7 XRD patterns of ZMNSs grown with 0.1 M precursor solution at 110 °C for 1, 2 and 4 hr duration on the: (a) Si substrate, (b) glass substrate, and (c) substrate dependent comparison for 3 hr growth duration 95
- 4.8 PL spectra of ZMNSs grown on glass and Si substrates for time duration of: (a) 1 hr, (b) 2 hr, (c) 3 hr, and (d) 4 hr. Dashed lines are the Gaussian fits 99
- 4.9 Growth time duration dependent variations of the PL peak positions for samples grown on glass and Si substrates 100
- 4.10 FESEM images showing ZNs film (sample L7) grown on Si substrate at 90 °C for 3 hr, pH 5.7 and 0.1 M: (a and b) enclosed tube- and solid rod-like ZNs, (c) enclosed tube-like ZNs and (d) solid rod-like ZNs 101
- 4.11 FESEM images showing ZNs film morphology (sample L8) grown on Si substrate at 90 °C for 3 hr, pH 5.7 and 0.01 M: (a and b) rice-, star rice- and flower rice-like, Insets dashed lines in image (b) are the flower rice-like ZNs, (c) FESEM magnified image of rice-, star rice- like ZNs, and (d) FESEM magnified image of rice-like ZNs tip 102
- 4.12 XRD patterns of ZNSs films grown on Si substrates for different precursor concentration of 0.01 to 0.1 M at 90 °C for 3 hr with pH 5.7 103
- 4.13 FTIR spectra of ZNSs films grown under various precursor concentrations (0.01-0.10 M) for 90 °C and 3 hr and pH 5.7 104
- 4.14 PL emission spectra of ZNSs films grown on Si substrates at 90 °C for 3 hr with pH 5.7 for varying nutrient molar concentration from 0.01 M

	to 0.1 M	105
4.15	FESEM images of high density ZNSs morphology (sample L9) grown on Si substrate at 90 °C for 3 hr, 0.1 M and pH 10.5: (a) flower-like ZNSs film and (b and c) FESEM images with closer view of flower-like ZNSs	106
4.16	XRD patterns of as-prepared ZNSs films on Si substrates deposited at 90 °C for 3 hr under varying nutrient pH range of 5.7 to 10.5	107
4.17	PL spectra of as-prepared ZNSs films grown on Si substrate at 90 °C for 3 hr with solution pH values of 5.7 and 10.5	108
4.18	FTIR spectra of ZNSs films grown with different pH of 5.7 to 10.5 at 90 °C for 3 hr duration	109
4.19	(a and b) FESEM images of as-synthesized ZNSs-based film on Si substrate at 110 °C for 3 hr, 0.1 M and pH 10.5. Red circles reveal the formation of multipods-like ZNs and (c) represent the high magnification of FESEM image (dotted circle) of flower-like ZNs	111
4.20	Schematic picture of a hexagonal ZnO crystal revealing different planes with polar planes (top and bottom ends) and others nonpolar planes	112
4.21	Schematic diagram of the growth mechanism for urchin-, flower-, and multipods-like ZMNSs	114
4.22	(a) HRTEM image of the ZnO NPs produced via laser ablation of the zinc target in water at 200 mJ, 10 Hz and 1000 pulses, and (b) size distribution of the corresponding sample containing ZNPs. The blue curve is the Gaussian fit (inset: the hexagonal ZnO structure)	117
4.23	(a-b) HRTEM images of ZNPs grown at 200 mJ, (c-d) corresponding single profile lattice	

	fringes of ZNP	118
4.24	(a) HRTEM image, and (b) histogram of size distribution of the ZnO NPs produced via PLAL technique with the zinc target at 400 mJ for 10 HZ and 1000 pulses. The blue curve is the Gaussian fit	119
4.25	(a) HRTEM image (b) enlarged of square area of ZNPs grown at 400 mJ, and (c and d) corresponding single profile lattice fringes of ZNPs. The red circle in (a) revealing the existence of hexagonal shaped ZNP	120
4.26	UV-Vis spectra of as-grown ZNPs colloidal solutions for different laser ablation energy (200 and 400 mJ)	121
4.27	FESEM images of sample S1 revealing four types of morphologies grown on Si substrate at 110 °C for 5 min with pH 10.5: (a) hollow flower-like, (b) taper-like, and (c) flower- and multipod-like. The ZNPs colloid solution is prepared at 200 mJ	124
4.28	ZnO nanotapers for four types of ZNSs grown on Si substrate at 110 °C for 5 min and pH 10.5: (a) lengths, and (b) diameters	125
4.29	FESEM images of ZNSs (sample S2) grown on Si substrate at (110 °C, 0.5 min and pH 10.5) with ZNPs colloid prepared at 200 mJ: (a and b) flower- and multipod-like ZNs, (c and d) FESEM images with high magnification of single flower-like ZNs with hollow centre (red circle)	126
4.30	FESEM images of ZNSs (sample S3) morphology grown on Si substrate at 110 °C for 60 min and pH 10.5. The ZNPs colloid prepared at 200 mJ: (a and b) dispersive and collapsing taper-like and hollow flower-like ZNSs-based film and (c and d)	

	FESEM magnified images of hollow flower-like ZNSs	127
4.31	FESEM images of sample L10 consisted of flower-like and multipod-like ZNSs deposited on Si substrate at (110 °C for 5 min and pH 10.5) by hydrothermal method: (A, B and C) flower-like and multipod-like ZNSs, (a and b) ZnO nanotaper with flat and sharp tips dependent flower-like and multipod-like ZNSs, and (c) FESEM image with high magnification of multipod-like ZNSs	129
4.32	Distribution of ZnO nanotaper dependent flower-like and multipod-like ZNSs for samples S1 and L10: (a) lengths, and (b) diameters	130
4.33	XRD patterns of the ZNSs grown on Si substrates for samples: (a) S1 and S2 samples grown via PLAL-H technique at different growth time (0.5-5.0 min), and (b) S1 and L10 samples grown using PLAL-H and hydrothermal technique	131
4.34	FTIR spectra of the as-grown S1, S2 and L10 ZNSs films	133
4.35	UV-Vis spectra of the as-grown ZNSs films for S1, S2 and L10 samples	135
4.36	Room temperature PL spectra of the as-grown ZNSs films for samples S1, S2 and L10	137
4.37	Schematic diagram illustrating the growth mechanism of the diverse ZNSs morphologies with various aspect ratios deposited on the Si substrate via PLAL-H technique: (a) multipod-like, flower-like, and hollow flower-like ZNSs and (b) taper-like, multipod-like, flower-like, and hollow flower-like ZNSs	141
4.38	(A) FESEM images of ZNSs (sample S4) deposited on Si substrate through employ colloidal	

- ZNPs prepared at (400 mJ), hydrothermal treatment is carried out at 110 °C for 5 min and pH 10.5: (a) FESEM magnification image of flower-like ZNs, (B-b) insets dashed lines are clarified for deformation and collapse of NRs dependent flower-like ZNs, and (C, c, D and d) magnified images are elucidated of ZNRs dependent flower-like ZNs embedded in ZnO nanowall 143
- 4.39 Histogram distribution of ZNRs dependent flower-like ZNs of samples S1 and S4 grown based on using colloidal ZNPs prepared for various ablation energy (200-400 mJ): (a) lengths and (b) diameters 144
- 4.40 XRD patterns of as-prepared ZNSs films (samples S1 and S4) grown on Si substrate using PLAL-H technique at 110 °C for 5 min and pH 10.5. Colloidal ZNPs prepared under various ablation energy (200-400 mJ) 145
- 4.41 FTIR spectra of as-synthesized ZNSs films for samples S1 and S4 grown on Si substrates via PLAL-H technique at 110 °C for 5 min and pH 10.5. Colloidal ZNPs prepared under various ablation energy (200-400 mJ) 146
- 4.42 PL spectra of as-prepared ZNSs films (samples S1 and S4) grown on Si substrates via PLAL-H technique at 110 °C for 5 min and pH 10.5. ZNPs colloids are prepared at different ablation energy (a) 200 mJ, and (b) 400 mJ 148
- 4.43 FESEM images of as-prepared ZNSs-based films (samples S5, S6 and S7) deposited on Si substrates at 110 °C, inherent pH 7.6 and different growth times (a-A) (5 min), (b-B) (30 min) and (c-C) (60 min), respectively. (a-A) rod- and flower-like

- ZNs, (b-B) irregular shaped disordered NRs, and (c-C) high density NRs comprising of NFs-like ZNSs possessed high aspect ratio. Insets (Figure 4.43(a-c)) are the closer view of ZNRs and ZNFs. The colloidal ZNPs produced by PLAL at (200 mJ) 150
- 4.44 Distribution of ZNRs dependent ZNSs grown on Si substrate at 110 °C, pH 7.6 and growth time of 60 min for: (a) lengths and (b) diameters fitted to the Gaussian 151
- 4.45 FESEM images of as-grown ZNSs-based films (samples S8, S9 and S10) deposited on Si substrates at 110 °C, pH 10.5 and different growth times (a-A) (5 min), (b-B) (30 min) and (c-C) (60 min), respectively. (a-A) independent rod- and tube-like ZNSs, (b-B) independent small spherical clusters and NSs collapsed, and (c-C) high density ZNPs. Inset in (a) and (C) displays the closer view of NRs and NPs diameter distribution, respectively. The colloidal ZNPs produced by PLAL at (200 mJ) 152
- 4.46 XRD patterns of rod/flower-like ZNs and ZNPs films, synthesized by PLAL-H technique under 110 °C for 60 min in the nutrient pH range of 7.6-10.5 154
- 4.47 Nutrient pH (7.6-10.5) value dependent FTIR spectra of ZNSs prepared using PLAL-H technique at 110 °C for 1 hr duration 155
- 4.48 Nutrient pH dependent PL spectra of as-synthesized ZNSs using PLAL-H method grown at 110 °C for 60 min 157
- 4.49 UV-Vis absorption spectra of as-prepared ZNSs (using PLAL-H technique under 110 °C for

	60 min) for different nutrient pH	159
4.50	Schematic illustration of the growth mechanism for different ZNSs by PLAL-H technique depending on various nutrient pH values (I) 7.6 and (II) 10.5 at growth temperature of 110 oC and growth time of 5, 30 and 60 min: (I-A) small petal-like ZNRs/ZNFs and (I-B) distinct ZNRs/ZNFs of higher density and aspect ratio; (II-a) rod- and tube-like ZNSs, (II-b) deformation and collapse of ZNSs and subsequent formation of independent small spherical clusters, and (II-c) ZNPs–based compact film	162
4.51	UV-Vis absorption spectra displaying the temporal evolution of photocatalytic decolouration of MB under solar irradiation for ZNSs grown by PLAL-H technique at nutrient pH of: (a) 7.6 for NRs/NFs-like ZNSs (sample S7) and (b) 10.5 for NPs-like ZNSs (sample S10)	165
4.52	Solar irradiation duration dependent photodegradation of MB dye for as-synthesized ZNSs grown by PLAL-H technique at different nutrient pH as well as photographs of photodegradation of MB suspensions (a) pH 10.5 and (b) pH 7.6	166
4.53	UV-Vis absorption spectra displaying the temporal evolution of photocatalytic decolorization of MB under solar irradiation for ZNSs grown by PLAL-H technique dependent ZNPs colloids prepared at various ablation energy of: (a) 200 mJ (sample S1), and (b) 400 mJ (sample S4)	169
4.54	Solar irradiation duration dependent photodegradation of MB dye for as-synthesized	

- ZNSs grown by PLAL-H technique dependent ZNPs colloids prepared at different ablation energy (200-400 mJ), as well as photographs of MB photo-degradation (a) 400 mJ and (b) 200 mJ 169
- 4.55 UV-Vis absorption spectra exhibiting the temporal evolution of photocatalytic decolorization of MB under solar irradiation for ZNSs films developed by traditional hydrothermal method at 110 °C, pH 10.5, 0.1 M and different growth times of: (a) 5 min (sample L10), and (b) 3 hr (sample L3) 170
- 4.56 Solar irradiation duration dependent photodegradation of MB dye for as-synthesized ZNSs developed by traditional hydrothermal method at 110 °C, pH 10.5, 0.1 M and different growth times of (5 to 3 hr), as well as photographs of MB photo-degradation (a) 5 min (sample L10), and (b) 3 hr (sample L3) 171
- 4.57 UV-Vis absorption spectra showing the temporal evolution of photocatalytic decolourization of MB under solar irradiation for ZNSs films grown by direct hydrothermal method at 90 °C for 3 hr, pH 5.7 and at various concentrations of: (a) 0.1 M (sample L7), and (b) 0.01 M (sample L8) 172
- 4.58 Solar irradiation duration dependent photodegradation of MB dye for as-synthesized ZNSs developed by traditional hydrothermal method at 90 °C for 3 hr and pH 5.7 under nutrient concentrations of (0.1 M and 0.01 M), as well as photographs of MB photo-degradation of: (a) 0.1 M (sample L7), and (b) 0.01 M (sample L8) 172

- 4.59 Histogram shows the photocatalytic efficiency of de-colorization of MB suspension under solar irradiation at different days for divers ZNSs films dependent growth techniques (hydrothermal and PLAL-H methods)

173

LIST OF ABBREVIATIONS

AOPs	-	Advanced Oxidation Processes
BSEs	-	Back-Scattered Electrons
CB	-	Conduction Band
CVD	-	Chemical Vapor Deposition
DW	-	Distilled Water
EDX	-	Energy Dispersive X-ray Diffraction
EDA	-	Ethylenediamine
FESEM	-	Field Emission Scanning Electron Microscopy
FTIR	-	Fourier-Transform Infrared
FTO	-	Fluorine-Doped Tin-Oxide-Coated Glass
IR	-	Infrared
ITO	-	Indium Tin Oxide
H	-	Hydrothermal
HRTEM	-	High Resolution Transmission Electron Microscopy
JCPDS	-	Joint Committee on Powder Diffraction Standards
MOCVD	-	Metal Organic Chemical Vapor Deposition
MBE	-	Molecular Beam Epitaxy
m-ZnO	-	Modified ZnO
NPs	-	Nanoparticles
NWs	-	Nanowires
NRs	-	Nanorods
NLs	-	Nanoleafs
NBs	-	Nanobelts
NCs	-	Nanocages
NFs	-	Nanoflowers
Nd:YAG	-	Neodymium-Doped Yttrium Aluminum Garnet

NIR	-	Near Infrared
NBE	-	Near Band Edge Emission
n-type	-	Donor Type
1D	-	One Dimension
O _i	-	Oxygen Interstitials
V _o	-	Oxygen Vacancies
O _{Zn}	-	Oxygen Antisites
PLD	-	Pulsed Laser Deposition
PLAL	-	Pulse Laser Ablation Under Liquid
PL	-	Photoluminescence
PVD	-	Physical Vapor Deposition
p-ZnO	-	Pure ZnO
PEs	-	Primary Electrons
QDs	-	Quantum Dots
QCEs	-	Quantum (Size) Confinement Effects
RT	-	Room Temperature
SEM	-	Scanning Electron Microscopy
SPR	-	Surface Plasmon Resonance
PLAL-H	-	Synergistic Effect of PLAL and Hydrothermal Methods
SEs	-	Secondary Electron
2D	-	Two Dimensions
3D	-	Three Dimensions
UV	-	Ultraviolet
Vis	-	Visible
VB	-	Valance Band
XRD	-	X-ray Diffraction
RF	-	Radio-Frequency
ZMNSs	-	ZnO Micro/Nanostructures
ZNSs	-	Zinc Oxide Nanostructures
ZNPs	-	Zinc Oxide Nanoparticles
ZNRs	-	Zinc Oxide Nanorods
ZNFs	-	Zinc Oxide Nanoflowers
0D	-	Zero Dimension

V_{Zn}	-	Zinc Vacancies
Zn_i	-	Zn Interstitials
Zn_o	-	Zn Antisites

LIST OF SYMBOLS

α	- Absorption Coefficient
\AA	- Angstrom
D	- Average Crystallite Size
Atm	- Atmosphere
NH_3	- Ammonia
I-V	- Current-Voltage
$^{\circ}\text{C}$	- Celsius (Degree Centigrade)
cm	- Centimeter
k	- Crystallite Shape-Dependent Scherrer's Constant
C_{mb}	- Concentration of MB After Irradiation Time (t).
Co	- Cobalt
Cu	- Copper
C	- Carbon
CO_2	- Carbon Dioxide
CdS	- Cadmium Sulfide
d	- Distance Between Atomic Layers
θ	- Diffraction Angle
δ	- Dislocation Density
eV	- Electron-Volt
e-h	- Electron-Hole
E_g	- Energy Band Gap
ν	- Frequency
β (FWHM)	- Full Width at Half-Maximum
6HCHO	- Formaldehyde
F	- Fluorine
Au	- Gold

hr	- Hour
Hz	- Hertz
H ₂ O ₂	- Hydrogen Peroxide
H ⁺	- Hydrogen (Cationic)
OH ⁻	- Hydroxide Ion
HO ₂ [•]	- Hydroperoxyl Radical
(CH ₂) ₆ N ₄ or HMT	- Hexamethylenetetramine
H ₂ O	- Water
<i>n</i>	- Order of Diffraction
Fe ₂ O ₃	- Iron Oxide
<i>C_o</i>	- Initial Concentration of MB
J	- Joule
mJ	- Milli-Joule
kV	- Kilo-Volt
K	- Kelvin
<i>k_B</i>	- Boltzmann Constant
<i>a</i> and <i>c</i>	- Lattice Constant
m	- Meter
mm	- Millimeter
μm	- Micrometer
nm	- Nanometer
min	- Minute
<i>hkl</i>	- Miller Indices
M	- Molarity
C ₁₆ H ₁₈ N ₃ SCl /MB	- Methylene Blue
ϵ	- Microstrain
N	- Nitrogen
NiO	- Nickel Oxide
O	- Oxygen
pH	- Potential of Hydrogen
Pa	- Pascal
kPa	- Kilopascal
GPa	- Gigapascal

ps	- Picosecond
ns	- Nanosecond
h	- Planck's Constant
Pt	- Platinum
$\eta\%$	- Percentage Photodegradation Efficiency
N1	- Precursor Solution
m_o	- Rest Mass of the Electron (9.110×10^{-31} kg)
SiO ₂	- Silicon Dioxide (Silica)
Si	- Silicon
Ag	- Silver
t	- Time
T	- Temperature
SnO ₂	- Tin Dioxide
TiO ₂	- Titanium Dioxide
WO ₃	- Tungsten Oxide
λ	- Wavelength
W	- Watt
ZnO	- Zinc Oxide
Zn	- Zinc
N2	- ZNPs Colloid
Zn(OH) ₂	- Zinc Hydroxide
Zn(NO ₃) ₂ .6H ₂ O	- Zinc Nitrate Hexahydrate
Zn(NO ₃) ₂	- Zinc Nitrate
ZrO ₂	- Zirconium Dioxide

LIST OF APPENDICES

APPENDIX	TITLE	PAGE
A	List of Publications	183

CHAPTER 1

INTRODUCTION

1.1 Overview

Richard Feynman (1959) first introduced the concept of “nanotechnology” in a seminar presentation entitled “*There’s Plenty of Room at the Bottom*” [1]. This notion was further extended by E. Drexler in a celebrated book titled “engines of creation: the coming era of nanotechnology” [1, 2]. Since then, several discoveries and inventions related to nanoscience and nanotechnology have made a significant impact in terms of potential applications. Presently, nanoscience is the frontier research topic in every frontier of science, technology and engineering. Intense efforts are made to achieve new functional nanomaterials for efficient, economic and environmental friendly applications. Nanotechnology involves materials or structures at length scales ranged between sub-nanometer to few hundreds of nanometer. Over the years, it is realized that properties of materials can be fine-tuned by changing the dimension (size and shape) without altering the chemical composition.

It is proven that the properties materials at nanoscale are very different from their bulk counterpart. The large surface area to volume ratio and the quantum confinement or quantum size effects make low dimensional distinct compared to bulk materials. For example, metals (e.g. Au and Ag) at nanoscale possess an enhanced absorption and scattering properties for visible light due to the influence of surface plasmon resonance (SPR) [3]. Whereas, semiconductors materials (e.g. ZnO

and TiO_2) at lower dimensions (nanometer size) show emerging optical and electronic structure properties due to quantum size effects. Several studies revealed that the effect of quantum confinement in semiconductor nanostructures appears more prominent at length scale comparable to exciton Bohr radius, where energy levels become quantized [4-6].

Nanotechnology offers diverse prospective applications in the field of optics, energy system, electronics, biomedicine, biology, environment, security, gas sensing etc. to cite a few [7]. Depending on the dimension of nanostructures, materials are categorized as zero dimensional (0D) called nanoparticle (NP), one dimensional (1D) called nanowire (NW) and nanorod (NR); two dimensional (2D) known as quantum well (QW) and three dimensional (3D) flower- and multipod- like nanostructures as shown in Figure 1.1 [8-10].

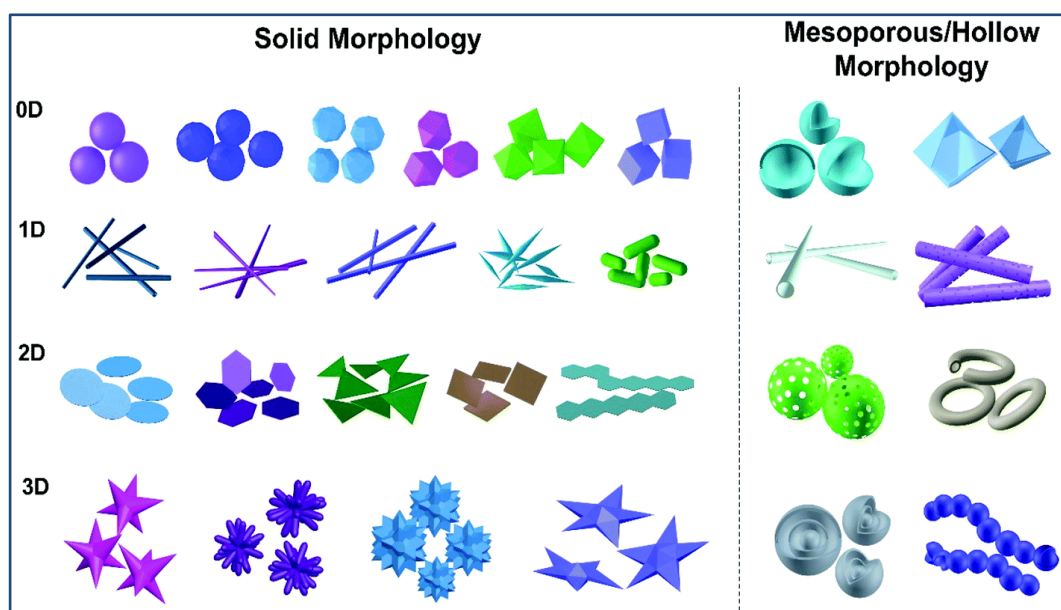


Figure 1.1 Overview of different structures and geometries at nanoscale [11]

Amongst various wide band-gap semiconductor nanomaterials, zinc oxide (ZnO) nanostructures (ZNSs) are very prospective in broad array of technological applications owing to their excellent electronic structure properties. Diverse

nanostructures of ZnO with unique features can easily be achieved using different synthesis methods. These nanostructures possess outstanding optical properties which are advantageous for the advancement of photovoltaic and optoelectronic nanodevices. Furthermore, control of ZnO epitaxial layer quality together with native and dopant point defects remains a vital issue for direct nanodevice production [12].

In the past, numerous techniques are developed for the production of diverse ZNSs under specific controlled growth conditions [12-17]. These methods include pulsed laser deposition (PLD), sol-gel processing, spray pyrolysis, electrochemical deposition, pulse laser ablation in liquid (PLAL), metal organic chemical vapour deposition (MOCVD), molecular beam epitaxy (MBE), radio-frequency (RF) sputtering, hydrothermal etc. Different techniques produce different kinds of ZNSs morphology such as ZNPs, ZNWs, ZNRs, ZnO nanoleafs (ZNLs), ZnO nanobelts (ZNBs), ZnO nanocages (ZNCs), ZnO nanoflowers (ZNFs) etc. Figure 1.2 shows the scanning electron microscope (SEM) images of different types of ZNSs grown via hydrothermal method.

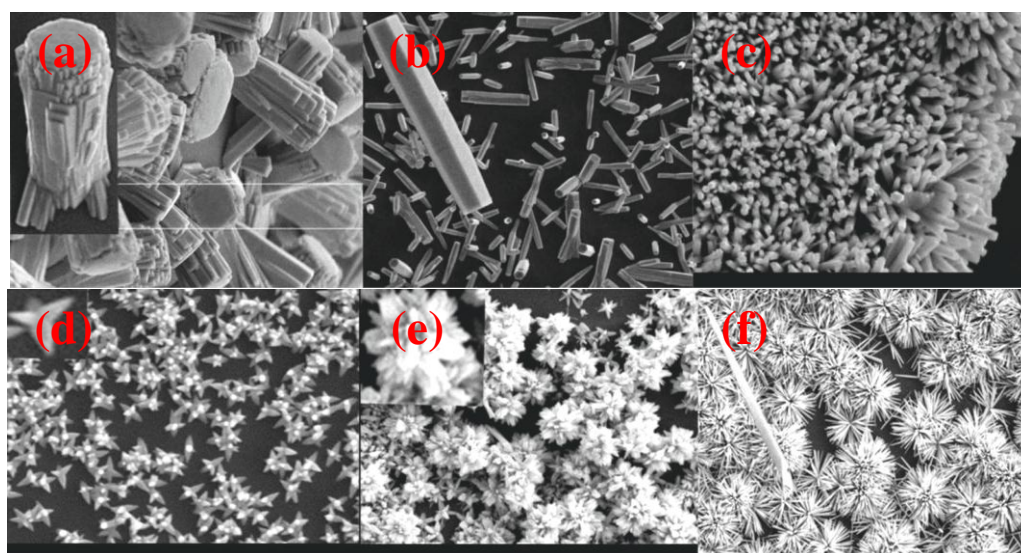


Figure 1.2 SEM images of various ZNSs synthesized on Si substrates using hydrothermal method: (a, b and c) rod-like, (d) star-like, and (e and f) flower-like [18]

Despite much progress in the preparation methods, controllable growth of ZNSs with desired properties are still demanding for several applications including electronics, optoelectronics, gas sensing, energy conversion/storage devices and photocatalysis [19-24]. Research revealed that the characteristics of produced ZNSs and their subsequent applications are critically decided by the nature of growth technique and the inter-play of different growth parameters (temperature, time, precursor type and concentration, seed layer, nutrient pH value etc.). All these parameters associated with the conventional growth techniques revealed their strong influence on the quality of ZNSs (morphology, structure quality, size, density, alignment, electrical and optical properties etc.) [25-27]. Earlier, many attempts are made to control the physical, structural, electrical and optical properties of ZNSs under mild growth conditions. The main aim was to determine the significant behaviors of ZNSs towards the advancement of novel and efficient nanodevices [13, 24, 28-30].

Among various methods of synthesis, both PLAL and hydrothermal (H) techniques have added advantages for the production of good quality ZNSs (undoped and doped) under mild growth conditions. Considering these notable merits, present thesis made a synergistic combination of the PLAL and hydrothermal methods (hereafter called PLAL-H technique) for the controlled growth of ZNSs with evolving morphologies. Using this novel method, varieties of ZNSs-based films are grown, which depended on the growth conditions including ablation energy mediated production of ZNPs colloids, substrate nature, growth temperature and time, precursor type and concentration, and nutrient pH values. Such growth conditions dependent ZNSs morphology, size, density and crystallinity, and optical properties are determined. Propose and understanding growth mechanisms processes are investigated. Furthermore, these as-synthesized ZNSs morphology driven improvement in the photocatalytic activity under sunlight irradiation is evaluated.

1.2 Photocatalytic Application

In recent time, freshwater pollution due to residual organic dyes emanating from the industries such as textile, pharmaceutical, pesticides, tannery, craft bleaching, cosmetic, food processing and agriculture is a major environmental concern (Figure 1.3). In fact, about 7×10^5 tonnes of organic dyes are annually produced worldwide in which more than 10-15% is leached into the wastewater during manufacturing and processing [31]. These chemicals are not only highly toxic and hazardous to the living organism but their intermediates can undergo reductive processes and result in the formation of potentially carcinogenic or mutagenic compounds unless inhibited. Thus, considering the toxicity potential of these dyes in the environment their immediate remediation before being discharging into the surroundings is mandatory.



Figure 1.3 Pictures showing the freshwater pollution (a and b) due to chemicals fallout and (c and d) its influence on the living organism [32]

In the past, diverse methods are developed to diminish the impact of such toxic chemical pollutants on the non-human environment, aquatic systems, and human life. Methods including adsorption, membrane separation and biological treatments are limited due to their high operating cost and inefficient in removing these pollutants. Currently, photocatalytic reactions based photodegradation processes have been introduced as an effective and economic strategy to eliminate such pollutants. In this regard, semiconductor nanomaterials (ZnO, SiO₂ and TiO₂) revealed great prospects for photocatalytic applications to treat the environmental pollutants. Categorically, heterogeneous photocatalysis-based ZNSs owing to their unusual attributes such as diverse morphologies, ability to absorb a wide solar spectrum, high chemical stabilizations, nontoxicity, abundance in nature and low cost became attractive. Thus, this material is chosen for the effective remediation of toxic environmental pollutants [19, 33, 34]. Many literature findings showed that the optimization of physical properties of as-synthesized ZNSs in terms of large surface area and modified bandgap can be useful for the increase of the number of active sites and subsequent charge transfer useful for enhanced photocatalytic activity. This in turn enhances the electron–hole pairs' separation efficiency in the photocatalytic reactions, resulting in the enhancement of the photocatalytic efficiency [19, 31, 34-36].

1.3 Problem Statement

Despite the development of various syntheses methods of ZNSs a controlled growth technique with mild conditions that produce evolving morphologies and desirable properties is far from being achieved. Controlled growths of ZNSs are significant for determining the overall properties as well as potential applications. Most of the existing synthesis methods have complicated conditions such as high vacuum, expensive devices, specialized laboratory, complex growth procedures, high temperature, requirement of catalyst or template, and longer growth time. It is necessary to develop a simple, fast, scalable, cost-effective and catalyst-free new growth approach such as PLAL-H (combination of PLAL and hydrothermal

methods). This novel technique is expected to achieve better control on the growth of ZNSs-based film, which is still lacking. A better understanding of the PLAL-H growth mechanism that produces ZNSs with evolving morphologies in addition to improved photocatalytic efficiency toward MB dye under sunlight irradiation is prerequisite.

Modifications in the photocatalytic activity of ZNSs for practical applications remain a major issue due to their wide band-gap nature and subsequent absorption in the UV region only. On top, the wide band-gap nature of ZNSs allows only ~ 4-5% of the solar spectrum in the UV-range for effective use as a renewable energy source, which is the main limitation for photocatalytic application. Furthermore, studies on superior photo-degradation ability of MB by un-doped ZNSs-based film under sunlight irradiation are rarely performed. Earlier studies mainly focused on ZNSs-based powder to achieve photodegradation of MB dye. These are not only expensive, but required complex processing tools such as centrifugation. Consequently, it is necessary to overcome the limitations associated with weak photocatalytic activities of ZNSs where an enhancement in the harvesting (absorption) efficiency of the solar spectra in the broad region (UV and visible (Vis) regions) and reduction of processing cost is necessary. In this view, present thesis took a fair attempt to develop a new PLAL-H growth technique for overcoming all the above mentioned limitations associated with the synthesis of ZNSs using conventional methods as well as the photocatalytic application of ZNSs driven by sunlight irradiation.

1.4 Research Objectives

Based on the aforementioned problem statement and research background on ZNSs the following objectives are set:

1. To develop a new PLAL-H technique with mild growth conditions for the controlled synthesis of ZNSs-based film having evolving morphologies.
2. To determine the influence of growth parameters on the morphology, size, density, structure, composition, optical properties and photocatalytic activities of the synthesized ZNSs-based film.
3. To evaluate the photocatalytic activity of the as-grown ZNSs-based films in terms of photo-degradation ability of MB under sunlight irradiation.

1.5 Scope of the Study

Present study includes the synthesis, characterization and determination of photocatalytic properties of ZNSs-based films. Amongst all the metal oxides semiconductors ZnO is preferred for various applications because of their distinct physical and chemical attributes including wide direct band gap, large exciton binding energy, excellent stability, environmental friendliness, low cost and easy availability. These fascinating properties are supported by ability of ZnO to easy formation of different nanostructures (ZNSs) gained high surface area to volume ratio and effective quantum confinement compared to bulk structure. Intense researches revealed the possibility of tuning the electronic band structure of ZnO via controlled synthesis of ZNSs useful for light-emitting diodes, sensors, catalysts, field emitters, biosensors, solar cell and photocatalytic application. Preparation of ZNSs-based films with controlled morphologies will be achieved via newly proposed PLAL-H growth technique as well as using conventional hydrothermal route to authenticate its ability for producing high quality ZNSs with diverse morphologies. The growth conditions optimization by varying different growth parameters would

be the major focus. The impact of various processing parameters including laser energy, nutrient type, nutrient pH, nutrient concentration, growth temperature and time on the ZNSs growth mechanism will be determined. Such NSs properties such as morphology, density, orientation, aspect ratio, crystal size and crystallinity are found to be strongly depended on the synthesis technique and processing conditions.

Current newly proposed simple PLAL-H technique is capable of controlling the morphology, aspect ratio, density, structure, optical and photocatalytic properties of ZNSs. This technique is cost-effective and can produce good quality ZNSs at short growth time and low temperature (under mild growth conditions) without requiring any catalysts. Moreover, more than three ZNSs can be grown simultaneously. Such ZNSs with diverse morphologies, sizes and crystallinity are essential for the development of ZNSs based optoelectronic devices which are cheap and efficient. Using the proposed systematic characterization method it is possible to determine the purity, size, emission and absorption properties, band gap, photocatalytic activity and morphology of ZNSs as well as other nanomaterials required for broad array of applications. The photocatalytic performance of the optimal ZNSs samples under sunlight irradiation will be measured in terms of photo-degradation of MB dye.

As-prepared samples are thoroughly characterized using various imaging and spectroscopic techniques. The experimental results on as-synthesized ZNSs are compared with similar existing findings for better understanding of the growth mechanisms. Samples structures and morphology (surface morphology, size, density, crystallinity, and elemental traces) are determined using field emission scanning electron microscopy (FESEM), X-ray diffraction (XRD) measurement, high resolution transmission electron microscopy (HRTEM), Energy dispersive X-ray diffraction (EDX) and Fourier-transform infrared (FTIR) spectroscopy. The optical properties of ZNSs samples are determined via photoluminescence (PL) spectroscopy and UV-Vis absorption spectroscopy.

1.6 Significance of the Study

Nowadays the pollution of freshwater due to the residual organic contaminants (dyes) in the form of chemical waste being the major environmental concern needs remediation. These chemical pollutants are highly toxic and harmful for the entire eco-system. Therefore, degradation of these organic contaminants is essential to circumvent the human health risks. In this view, ZNSs-based films grown via innovative PLAL-H route can be superior in terms of photocatalytic efficiency toward pollutant MB dye under sunlight irradiation. This study is expected to contribute towards the development of high performing ZNSs with excellent photocatalytic activity under sunlight irradiation which is a free, clean, and inexhaustible irradiation source. The capacity to use ZNSs-based films for useful exploitation of sunlight source to achieve enhanced photocatalytic action would certainly be beneficial in terms of economy and environment. Furthermore, PLAL-H technique can be extended for producing other semiconductor NSs morphologies. Present PLAL-H technique may constitute a basis for controlled manipulation of nanomaterials desirable for high performance nanodevices.

1.7 Thesis Organization

This thesis is composed into five chapters as follows:

Chapter 1 presents a brief background of the research to justify the importance of ZNSs and need for further studies. It clearly shows the research gap to set out the precise objectives to be accomplished. It includes the problem statement, research objectives, scope, and significance.

Chapter 2 describes the comprehensive literature survey to show the existing research gaps and the relevant findings on the cited topic made so far. It describes the

electrical, optical and structural properties of ZnO nanostructure. It explains the growth mechanism of ZNSs associated with the hydrothermal and PLAL synthesis techniques. Influence of growth technique and growth conditions on the morphology of ZNSs films are discussed. The mechanism of photocatalytic activity of ZNSs is underscored. The major parameters of different growth techniques that can achieve enhanced photocatalytic efficiency of ZNSs film are explained in depth.

Chapter 3 highlights the detailed research methodology in terms of synthesis techniques used and the adopted steps towards photocatalytic applications. The background information of major experimental techniques for collecting the data and analysis related to as-grown ZNSs samples are emphasized.

Chapter 4 presents detailed results, analysis and discussion. Findings from two different synthesis methods such as hydrothermal and PLAL-H are evaluated in terms of optimization of growth conditions to produce various catalyst-free ZNSs films at low temperature and growth time compared with previous studies. The remarkable features of the synergistic PLAL-H technique for controlled preparation of ZNSs-based film are explained. Photocatalytic performance of obtained optimal ZNSs samples under sunlight irradiation is assessed using photodegradation of MB dye. Dependence of photodegradation efficiency of MB dyes on morphology and structure evolution of as-grown ZNSs films as well as ability of these ZNSs film as photocatalysis to overcome the shortcomings for beneficial exploiting of sunlight source is attributed.

Chapter 5 concludes the thesis and provides some future outlook in terms of recommendations. The successful accomplishments of the proposed research objectives are demonstrated.

REFERENCES

1. Corbett, J., P. McKeown, G. Peggs and R. Whatmore. Nanotechnology: international developments and emerging products. *CIRP Annals-Manufacturing Technology*. 2000. 49(2): 523-545.
2. Drexler, K. E. and M. Minsky. *Engines of creation*: Fourth Estate London. 1990.
3. Louis, C. and O. Pluchery. *Gold nanoparticles for physics, chemistry and biology*: World Scientific. 2012.
4. Senger, R. and K. Bajaj. Optical properties of confined polaronic excitons in spherical ionic quantum dots. *Physical Review B*. 2003. 68(4): 045313-1-045313-19.
5. Bawendi, M. G., P. Carroll, W. L. Wilson and L. Brus. Luminescence properties of CdSe quantum crystallites: Resonance between interior and surface localized states. *The Journal of Chemical Physics*. 1992. 96(2): 946-954.
6. Reimann, S. M. and M. Manninen. Electronic structure of quantum dots. *Reviews of Modern Physics*. 2002. 74(4): 1283-1298.
7. Djurišić, A. B. and Y. H. Leung. Optical properties of ZnO nanostructures. *Small*. 2006. 2(8-9): 944-961.
8. Cao, G. *Nanostructure and nanomaterials synthesis, properties and applications*: World Scientific. 2004.
9. Wang, N., Y. Yang and G. Yang. Great blue-shift of luminescence of ZnO nanoparticle array constructed from ZnO quantum dots. *Nanoscale Research Letters*. 2011. 6(1): 1-6.
10. Vanalakar, S. A., V. L. Patil, N. S. Harale, S. A. Vhanalakar, M. G. Gang, J. Y. Kim, P. S. Patil and J. H. Kim. Controlled growth of ZnO nanorod arrays

- via wet chemical route for NO₂ gas sensor applications. *Sensors and Actuators B: Chemical*. 2015. 221: 1195-1201.
11. Wu, Z., S. Yang and W. Wu. Shape control of inorganic nanoparticles from solution. *Nanoscale*. 2016. 8(3): 1237-1259.
 12. Willander, M. *Zinc Oxide Nanostructures: Advances and Applications*: CRC Press. 2014.
 13. Baruah, S. and J. Dutta. Hydrothermal growth of ZnO nanostructures. *Science and Technology of Advanced Materials*. 2009. 10(1): 013001-1-013001-18.
 14. Shi, F. and C. Xue. Morphology and growth mechanism of multileg ZnO nanostructures by chemical vapor deposition. *CrystEngComm*. 2012. 14(12): 4173-4175.
 15. Talebian, N., M. R. Nilforoushan and N. Maleki. Ultraviolet to visible-light range photocatalytic activity of ZnO films prepared using sol-gel method: The influence of solvent. *Thin Solid Films*. 2013. 527: 50-58.
 16. Feng, J. J., Q. C. Liao, A. J. Wang and J. R. Chen. Mannite supported hydrothermal synthesis of hollow flower-like ZnO structures for photocatalytic applications. *CrystEngComm*. 2011. 13(12): 4202-4210.
 17. Zhu, B., X. Zhao, F. Su, G. Li, X. Wu, J. Wu, R. Wu and J. Liu. Structural and optical properties of ZnO thin films on glass substrate grown by laser-ablating Zn target in oxygen atmosphere. *Physica B: Condensed Matter*. 2007. 396(1): 95-101.
 18. Amin, G., M. Asif, A. Zainelabdin, S. Zaman, O. Nur and M. Willander. Influence of pH, precursor concentration, growth time, and temperature on the morphology of ZnO nanostructures grown by the hydrothermal method. *Journal of Nanomaterials*. 2011. 2011: 269692-5- 269692-9.
 19. Kuriakose, S., B. Satpati and S. Mohapatra. Enhanced photocatalytic activity of Co doped ZnO nanodisks and nanorods prepared by a facile wet chemical method. *Physical Chemistry Chemical Physics*. 2014. 16(25): 12741-12749.
 20. Zhou, Y., D. Li, X. Zhang, J. Chen and S. Zhang. Facile synthesis of ZnO micro-nanostructures with controllable morphology and their applications in dye-sensitized solar cells. *Applied Surface Science*. 2012. 261: 759-763.
 21. Öztürk, S., N. Kılınc, N. Taştaltın and Z. Öztürk. A comparative study on the NO₂ gas sensing properties of ZnO thin films, nanowires and nanorods. *Thin Solid Films*. 2011. 520(3): 932-938.

22. Sun, X., Q. Li, J. Jiang and Y. Mao. Morphology-tunable synthesis of ZnO nanoforest and its photoelectrochemical performance. *Nanoscale*. 2014. 6(15): 8769-8780.
23. Peng, C., J. Guo, W. Yang, C. Shi, M. Liu, Y. Zheng, J. Xu, P. Chen, T. Huang and Y. Yang. Synthesis of three-dimensional flower-like hierarchical ZnO nanostructure and its enhanced acetone gas sensing properties. *Journal of Alloys and Compounds*. 2016. 654: 371-378.
24. Ansari, S. A., M. M. Khan, S. Kalathil, A. Nisar, J. Lee and M. H. Cho. Oxygen vacancy induced band gap narrowing of ZnO nanostructures by an electrochemically active biofilm. *Nanoscale*. 2013. 5(19): 9238-9246.
25. Schmidt-Mende, L. and J. L. MacManus-Driscoll. ZnO–nanostructures, defects, and devices. *Materials Today*. 2007. 10(5): 40-48.
26. Riedel, W., Y. Fu, Ü. Aksünger, J. Kavalakkatt, C. H. Fischer, M. C. Lux-Steiner and S. Gledhill. ZnO and ZnS nanodots deposited by spray methods: A versatile tool for nucleation control in electrochemical ZnO nanorod array growth. *Thin Solid Films*. 2015. 589: 327-330.
27. Hynek, J., V. Kalousek, R. Žouželka, P. Bezdička, P. Dzik, J. í. Rathouský, J. Demel and K. Lang. High photocatalytic activity of transparent films composed of ZnO nanosheets. *Langmuir*. 2014. 30(1): 380-386.
28. Heo, S. N., K. Y. Park, Y. J. Seo, F. Ahmed, M. Anwar and B. H. Koo. Effect of solution concentration on the functional properties of ZnO nanostructures: Role of Hexamethylenetetramine. *Electronic Materials Letters*. 2013. 9(3): 261-265.
29. Dedova, T., M. Krunk, I. O. Acik, D. Klauson, O. Volobujeva and A. Mere. Hierarchical nanostructures of ZnO obtained by spray pyrolysis. *Materials Chemistry and Physics*. 2013. 141(1): 69-75.
30. Tang, J. F., H. H. Su, Y. M. Lu and S. Y. Chu. Controlled growth of ZnO nanoflowers on nanowall and nanorod networks via a hydrothermal method. *CrystEngComm*. 2014. 17(3): 592-597.
31. Lam, S. M., J. C. Sin, A. Z. Abdullah and A. R. Mohamed. Degradation of wastewaters containing organic dyes photocatalysed by zinc oxide: a review. *Desalination and Water Treatment*. 2012. 41(1-3): 131-169.
32. Rana, S. *Environmental pollution: health and toxicology*: Alpha Science International Limited. 2006.

33. Hoffmann, M. R., S. T. Martin, W. Choi and D. W. Bahnemann. Environmental applications of semiconductor photocatalysis. *Chemical Reviews*. 1995. 95(1): 69-96.
34. Lee, K. M., C. W. Lai, K. S. Ngai and J. C. Juan. Recent developments of zinc oxide based photocatalyst in water treatment technology: a review. *Water Research*. 2016. 88: 428-448.
35. Sun, J. H., S. Y. Dong, J. L. Feng, X. J. Yin and X. C. Zhao. Enhanced sunlight photocatalytic performance of Sn-doped ZnO for Methylene Blue degradation. *Journal of Molecular Catalysis A: Chemical*. 2011. 335(1): 145-150.
36. Mohan, R., K. Krishnamoorthy and S. J. Kim. Enhanced photocatalytic activity of Cu-doped ZnO nanorods. *Solid State Communications*. 2012. 152(5): 375-380.
37. Fierro, J. L. G. *Metal oxides: chemistry and applications*: CRC press. 2005
38. Yano, M., K. Koike, S. Sasa and M. Inoue. *Zinc Oxide, Bulk, Thin Films and Nanostructures*. Elsevier Science. 2006: 372-414.
39. Noriega, R., J. Rivnay, L. Goris, D. Käblein, H. Klauk, K. Kern, L. M. Thompson, A. C. Palke, J. F. Stebbins and J. R. Jokisaari. Probing the electrical properties of highly-doped Al: ZnO nanowire ensembles. *Journal of Applied Physics*. 2010. 107(7): 074312-1-074312-8.
40. Choi, H. H. *Synthesis and characterization of tailored zinc oxide nanostructures and their engineered nanocomposites*. Thesis Doctor Philosophy. University of Florida. 2004.
41. Huh, P., F. Yan, L. Li, M. Kim, R. Mosurkal, L. A. Samuelson and J. Kumar. Simple fabrication of zinc oxide nanostructures. *Journal of Materials Chemistry*. 2008. 18(6): 637-639.
42. Xiaowei, S. and Y. Yang. *ZnO Nanostructures and Their Applications*: CRC Press. 2016.
43. Wang, Z. L. Zinc oxide nanostructures: growth, properties and applications. *Journal of Physics: Condensed Matter*. 2004. 16(25): R829.
44. Chen, Z., Z. Shan, S. Li, C. Liang and S. X. Mao. A novel and simple growth route towards ultra-fine ZnO nanowires. *Journal of Crystal growth*. 2004. 265(3): 482-486.

45. Li, S., X. Zhang, B. Yan and T. Yu. Growth mechanism and diameter control of well-aligned small-diameter ZnO nanowire arrays synthesized by a catalyst-free thermal evaporation method. *Nanotechnology*. 2009. 20(49): 495604-1-495604-9.
46. Özgür, Ü., Y. I. Alivov, C. Liu, A. Teke, M. Reshchikov, S. Doğan, V. Avrutin, S. J. Cho and H. Morkoc. A comprehensive review of ZnO materials and devices. *Journal of Applied Physics*. 2005. 98(4): 041301-1-041301-5.
47. Gil, B. and A. V. Kavokin. Giant exciton-light coupling in ZnO quantum dots. *Applied Physics Letters*. 2002. 81(4): 748-750.
48. Wong, E. M. and P. C. Searson. ZnO quantum particle thin films fabricated by electrophoretic deposition. *Applied Physics Letters*. 1999. 74(20): 2939-2941.
49. Gorla, C., W. Mayo, S. Liang and Y. Lu. Structure and interface-controlled growth kinetics of ZnAl₂O₄ formed at the (1120) ZnO/(0112) Al₂O₃ interface. *Journal of Applied Physics*. 2000. 87(8): 3736-3743.
50. Abbas, K. N., N. Bidin and R. S. Sabry. Controllable ZnO Nanostructures Evolution via Synergistic Pulsed Laser Ablation and Hydrothermal Methods. *Ceramics International*. 2016. 42: 13535-13546.
51. Bera, A. and D. Basak. Role of defects in the anomalous photoconductivity in ZnO nanowires. *Applied Physics Letters*. 2009. 94(16): 163119-1-163119-4.
52. Janotti, A. and C. G. Van de Walle. Fundamentals of zinc oxide as a semiconductor. *Reports on Progress in Physics*. 2009. 72(12): 126501-1-126501-29.
53. Epie, E. and W. Chu. Ionoluminescence study of Zn⁻ and O⁻ implanted ZnO crystals: An additional perspective. *Applied Surface Science*. 2016. 371: 28-34.
54. Fang, Y., Y. Wang, L. Gu, R. Lu and J. Sha. Effect of the defect on photoluminescence property of Al-coated ZnO nanostructures. *Optics Express*. 2013. 21(3): 3492-3500.
55. Liang, Y. C. and H. Zhong. Self-catalytic crystal growth, formation mechanism, and optical properties of indium tin oxide nanostructures. *Nanoscale Research Letters*. 2013. 8(1): 1-10.
56. Eason, R. *Pulsed laser deposition of thin films: applications-led growth of functional materials*: John Wiley and Sons. 2007.

57. Xiao, Q., J. Zhang, C. Xiao and X. Tan. Photocatalytic decolorization of methylene blue over $Zn_{1-x}Co_xO$ under visible light irradiation. *Materials Science and Engineering: B*. 2007. 142(2): 121-125.
58. Fan, Z. and J. G. Lu. Zinc oxide nanostructures: synthesis and properties. *Journal of Nanoscience and Nanotechnology*. 2005. 5(10): 1561-1573.
59. Zeng, H., X. W. Du, S. C. Singh, S. A. Kulinich, S. Yang, J. He and W. Cai. Nanomaterials via laser ablation/irradiation in liquid: a review. *Advanced Functional Materials*. 2012. 22(7): 1333-1353.
60. Kumar, R., G. Kumar and A. Umar. Pulse laser deposited nanostructured ZnO thin films: A review. *Journal of Nanoscience and Nanotechnology*. 2014. 14(2): 1911-1930.
61. Ishikawa, Y., Y. Shimizu, T. Sasaki and N. Koshizaki. Preparation of zinc oxide nanorods using pulsed laser ablation in water media at high temperature. *Journal of Colloid and Interface Science*. 2006. 300(2): 612-615.
62. Fazio, E., A. Mezzasalma, G. Mondio, F. Neri and R. Saija. ZnO nanostructures produced by laser ablation in water: optical and structural properties. *Applied Surface Science*. 2013. 272: 30-35.
63. Zeng, H., S. Yang and W. Cai. Reshaping formation and luminescence evolution of ZnO quantum dots by laser-induced fragmentation in liquid. *The Journal of Physical Chemistry C*. 2011. 115(12): 5038-5043.
64. Osuwa, J. and P. Anusionwu. Some advances and prospects in nanotechnology: a review. *Asian Journal of Information Technology*. 2011. 10: 96-100.
65. Zeng, H., Z. Li, W. Cai, B. Cao, P. Liu and S. Yang. Microstructure control of Zn/ZnO core/shell nanoparticles and their temperature-dependent blue emissions. *The Journal of Physical Chemistry B*. 2007. 111(51): 14311-14317.
66. Yang, G. *Laser ablation in liquids: principles and applications in the preparation of nanomaterials*: CRC Press. 2012.
67. Badawy, M. I., F. Mahmoud, A. A. Abdel-Khalek, T. A. Gad-Allah and A. Abdel Samad. Solar photocatalytic activity of sol-gel prepared Ag-doped ZnO thin films. *Desalination and Water Treatment*. 2014. 52(13-15): 2601-2608.

68. Russo, R., X. Mao, C. Liu and J. Gonzalez. Laser assisted plasma spectrochemistry: laser ablation. *Journal of Analytical Atomic Spectrometry*. 2004. 19(9): 1084-1089.
69. Mei, T. and Y. Hu. *Synthesis, Self-assembly and Optoelectronic Properties of Monodisperse ZnO Quantum Dots*: Intech Open Access Publisher. 2011.
70. Phipps, C. *Laser ablation and its applications*, ed. Vol. 129: Springer. 2007.
71. Guillén, G. G., M. M. Palma, B. Krishnan, D. Avellaneda, G. Castillo, T. D. Roy and S. Shaji. Structure and morphologies of ZnO nanoparticles synthesized by pulsed laser ablation in liquid: Effects of temperature and energy fluence. *Materials Chemistry and Physics*. 2015. 162: 561-570.
72. Yan, Z. and D. B. Chrisey. Pulsed laser ablation in liquid for micro-/nanostructure generation. *Journal of Photochemistry and Photobiology C: Photochemistry Reviews*. 2012. 13(3): 204-223.
73. Yang, G. Laser ablation in liquids: applications in the synthesis of nanocrystals. *Progress in Materials Science*. 2007. 52(4): 648-698.
74. Premkumar, T., P. Manoravi, B. Panigrahi and K. Baskar. Particulate assisted growth of ZnO nanorods and microrods by pulsed laser deposition. *Applied Surface Science*. 2009. 255(15): 6819-6822.
75. Zhang, X., H. Zeng and W. Cai. Laser power effect on morphology and photoluminescence of ZnO nanostructures by laser ablation in water. *Materials Letters*. 2009. 63(2): 191-193.
76. Thareja, R. and S. Shukla. Synthesis and characterization of zinc oxide nanoparticles by laser ablation of zinc in liquid. *Applied Surface Science*. 2007. 253(22): 8889-8895.
77. Tripathi, S., R. Choudhary, A. Tripathi, V. Baranwa, A. Pandey, J. Gerlach, C. Dar and D. Kanjilal. Studies of effect of deposition parameters on the ZnO films prepared by PLD. *Nuclear Instruments and Methods in Physics Research Section B: Beam Interactions with Materials and Atoms*. 2008. 266(8): 1533-1536.
78. Svetlichnyi, V., A. Shabalina, I. Lapin, D. Goncharova and A. Nemyokina. ZnO nanoparticles obtained by pulsed laser ablation and their composite with cotton fabric: Preparation and study of antibacterial activity. *Applied Surface Science*. 2016. 372: 20-29.

79. Camarda, P., R. Schneider, R. Popescu, L. Vaccaro, F. Messina, G. Buscarino, S. Agnello, F. Gelardi and M. Cannas. Effect of thermal annealing on the luminescence of defective ZnO nanoparticles synthesized by pulsed laser ablation in water. *Physica Status Solidi (C)*. 2016. 13(10-12): 890-894.
80. Hamad, A., L. Li and Z. Liu. Comparison of characteristics of selected metallic and metal oxide nanoparticles produced by picosecond laser ablation at 532 and 1064 nm wavelengths. *Applied Physics A*. 2016. 122(10): 904-1-904-15.
81. Goto, T., M. Honda, S. A. Kulinich, Y. Shimizu and T. Ito. Defects in ZnO nanoparticles laser-ablated in water-ethanol mixtures at different pressures. *Japanese Journal of Applied Physics*. 2015. 54(7): 070305-1-070305-6.
82. Hussain, M. Z., R. Khan, R. Ali and Y. Khan. Optical properties of laser ablated ZnO nanoparticles prepared with Tween-80. *Materials Letters*. 2014. 122: 147-150.
83. Solati, E., L. Dejam and D. Dorrnian. Effect of laser pulse energy and wavelength on the structure, morphology and optical properties of ZnO nanoparticles. *Optics and Laser Technology*. 2014. 58: 26-32.
84. Soliman, W., N. Takada, N. Koshizaki and K. Sasaki. Structure and size control of ZnO nanoparticles by applying high pressure to ambient liquid in liquid-phase laser ablation. *Applied Physics A*. 2013. 110(4): 779-783.
85. Kim, K. K., D. Kim, S. K. Kim, S. M. Park and J. K. Song. Formation of ZnO nanoparticles by laser ablation in neat water. *Chemical Physics Letters*. 2011. 511(1): 116-120.
86. Zeng, J. N., J. K. Low, Z. M. Ren, T. Liew and Y. F. Lu. Effect of deposition conditions on optical and electrical properties of ZnO films prepared by pulsed laser deposition. *Applied Surface Science*. 2002. 197: 362-367.
87. Fan, X., J. Lian, Z. Guo and H. Lu. ZnO thin film formation on Si (111) by laser ablation of Zn target in oxygen atmosphere. *Journal of Crystal Growth*. 2005. 279(3): 447-453.
88. Sasaki, T., Y. Shimizu and N. Koshizaki. Preparation of metal oxide-based nanomaterials using nanosecond pulsed laser ablation in liquids. *Journal of Photochemistry and Photobiology A: Chemistry*. 2006. 182(3): 335-341.
89. Feng, Z. C. *Handbook of Zinc Oxide and Related Materials: Volume Two, Devices and Nano-Engineering*, ed. Vol. 2: CRC Press. 2012.

90. Chen, M. Z., W. S. Chen, S. C. Jeng, S. H. Yang and Y. F. Chung. Liquid crystal alignment on zinc oxide nanowire arrays for LCDs applications. *Optics Express*. 2013. 21(24): 29277-29282.
91. Shen, G., P. C. Chen, K. Ryu and C. Zhou. Devices and chemical sensing applications of metal oxide nanowires. *Journal of Materials Chemistry*. 2009. 19(7): 828-839.
92. Lee, C. Y., S. Y. Li, P. Lin and T. Y. Tseng. ZnO nanowires hydrothermally grown on PET polymer substrates and their characteristics. *Journal of Nanoscience and Nanotechnology*. 2005. 5(7): 1088-1094.
93. Byrappa, K. and M. Yoshimura. Handbook of Hydrothermal Technology. A Technology for Crystal Growth and Materials Processing. *Byrappa, M. Yoshimura-Noyes Publications, Park Ridge, NJ*. 2001.
94. Motevalizadeh, L., Z. Heidary and M. E. Abrishami. Facile template-free hydrothermal synthesis and microstrain measurement of ZnO nanorods. *Bulletin of Materials Science*. 2014. 37(3): 397-405.
95. Guo, W., T. Liu, L. Huang, H. Zhang, Q. Zhou and W. Zeng. HMT assisted hydrothermal synthesis of various ZnO nanostructures: Structure, growth and gas sensor properties. *Physica E: Low-Dimensional Systems and Nanostructures*. 2011. 44(3): 680-685.
96. Öztürk, S., N. Kılınc, İ. Torun, A. Kösemen, Y. Şahin and Z. Z. Öztürk. Hydrogen sensing properties of ZnO nanorods: Effects of annealing, temperature and electrode structure. *International Journal of Hydrogen Energy*. 2014. 39(10): 5194-5201.
97. Sambath, K., M. Saroja, M. Venkatachalam, K. Rajendran and K. Jagatheeswaran. Hydrothermal Synthesis of Flower-Like ZnO Nanostructures and their Optical Properties. *Advanced Materials Research*. 2013. 678: 91-96.
98. Zhou, Q., W. Chen, S. Peng and W. Zeng. Hydrothermal synthesis and acetylene sensing properties of variety low dimensional zinc oxide nanostructures. *The Scientific World Journal*. 2014: 489170-1-489170-8.
99. Wang, H., J. Xie, K. Yan and M. Duan. Growth mechanism of different morphologies of ZnO crystals prepared by hydrothermal method. *Journal of Materials Science and Technology*. 2011. 27(2): 153-158.

100. Chakraborty, S. and P. Kumbhakar. Observation of bandgap narrowing effect and photoluminescence emission characteristics of chemically synthesized Co doped ZnO nanosheets. *Indian Journal of Physics*. 2014. 88(3): 251-257.
101. Kim, H. and K. Yong. A highly efficient light capturing 2D (nanosheet)-1D (nanorod) combined hierarchical ZnO nanostructure for efficient quantum dot sensitized solar cells. *Physical Chemistry Chemical Physics*. 2013. 15(6): 2109-2116.
102. Zhang, Y., H. Wang, H. Jiang and X. Wang. Water induced protonation of amine-terminated micelles for direct syntheses of ZnO quantum dots and their cytotoxicity towards cancer. *Nanoscale*. 2012. 4(11): 3530-3535.
103. Li, H., S. Jiao, S. Gao, H. Li and L. Li. Dynamically controlled synthesis of different ZnO nanostructures by a surfactant-free hydrothermal method. *CrystEngComm*. 2014. 16(38): 9069-9074.
104. Yang, L., P. W. May, L. Yin and T. B. Scott. Growth of self-assembled ZnO nanoleaf from aqueous solution by pulsed laser ablation. *Nanotechnology*. 2007. 18(21): 215602-1-215602-8.
105. Son, N. T., J.-S. Noh and I.-H. Lee. Low-temperature solution syntheses of hexagonal ZnO nanorods and morphology-controlled nanostructures. *Chemical Physics Letters*. 2016. 646: 185-189.
106. Guo, Y., S. Lin, X. Li and Y. Liu. Amino acids assisted hydrothermal synthesis of hierarchically structured ZnO with enhanced photocatalytic activities. *Applied Surface Science*. 2016. 384: 83-91.
107. Harish, S., M. Navaneethan, J. Archana, A. Silambarasan, S. Ponnusamy, C. Muthamizhchelvan and Y. Hayakawa. Controlled synthesis of organic ligand passivated ZnO nanostructures and their photocatalytic activity under visible light irradiation. *Dalton Transactions*. 2015. 44(22): 10490-10498.
108. Zhou, Y., C. Liu, X. Zhong, H. Wu, M. Li and L. Wang. Simple hydrothermal preparation of new type of sea urchin-like hierarchical ZnO micro/nanostructures and their formation mechanism. *Ceramics International*. 2014. 40(7): 10415-10421.
109. Shi, R., P. Yang, X. Dong, Q. Ma and A. Zhang. Growth of flower-like ZnO on ZnO nanorod arrays created on zinc substrate through low-temperature hydrothermal synthesis. *Applied Surface Science*. 2013. 264: 162-170.

110. Chen, P., L. Gu, X. Xue, Y. Song, L. Zhu and X. Cao. Facile synthesis of highly uniform ZnO multipods as the supports of Au and Ag nanoparticles. *Materials Chemistry and Physics*. 2010. 122(1): 41-48.
111. Mun, D. H., S. Bak, J. S. Ha, H. J. Lee, J. Lee, S. Lee and Y. Moon. Effects of precursor concentration on the properties of ZnO nanowires grown on (1–102) R-Plane sapphire substrates by hydrothermal synthesis. *Journal of Nanoscience and Nanotechnology*. 2014. 14(8): 5970-5975.
112. Pawar, R. C., H. Kim and C. S. Lee. Defect-controlled growth of ZnO nanostructures using its different zinc precursors and their application for effective photodegradation. *Current Applied Physics*. 2014. 14(4): 621-629.
113. Song, J. and S. Lim. Effect of seed layer on the growth of ZnO nanorods. *The Journal of Physical Chemistry C*. 2007. 111(2): 596-600.
114. Zhang, X., J. Qin, Y. Xue, P. Yu, B. Zhang, L. Wang and R. Liu. Effect of aspect ratio and surface defects on the photocatalytic activity of ZnO nanorods. *Scientific Reports*. 2014. 4: 4596-1-4596-8.
115. Yang, B., X. Zuo, X. Yang, L. Zhou and G. Li. Effects of pH values on crystal growth and photoluminescence properties of ZnO hexagonal rods with cones. *Materials Letters*. 2014. 130: 123-126.
116. Wahab, R., S. Ansari, Y. S. Kim, M. Song and H. S. Shin. The role of pH variation on the growth of zinc oxide nanostructures. *Applied Surface Science*. 2009. 255(9): 4891-4896.
117. Samaele, N., P. Amornpitoksuk and S. Suwanboon. Effect of pH on the morphology and optical properties of modified ZnO particles by SDS via a precipitation method. *Powder Technology*. 2010. 203(2): 243-247.
118. Tong, Y., Y. Liu, L. Dong, D. Zhao, J. Zhang, Y. Lu, D. Shen and X. Fan. Growth of ZnO nanostructures with different morphologies by using hydrothermal technique. *The Journal of Physical Chemistry B*. 2006. 110(41): 20263-20267.
119. Giri, P., S. Dhara and R. Chakraborty. Effect of ZnO seed layer on the catalytic growth of vertically aligned ZnO nanorod arrays. *Materials Chemistry and Physics*. 2010. 122(1): 18-22.
120. Peiris, T. N., H. Alessa, J. S. Sagu, I. A. Bhatti, P. Isherwood and K. U. Wijayantha. Effect of ZnO seed layer thickness on hierarchical ZnO nanorod

- growth on flexible substrates for application in dye-sensitised solar cells. *Journal of Nanoparticle Research*. 2013. 15(12): 1-10.
121. Kozuka, Y., A. Tsukazaki and M. Kawasaki. Challenges and opportunities of ZnO-related single crystalline heterostructures. *Applied Physics Reviews*. 2014. 1(1): 011303-1-011303-18.
122. Hai-Bo, F., Z. Xin-Liang, W. Si-Cheng, L. Zhi-Gang and Y. He-Bao. Zn/O ratio and oxygen chemical state of nanocrystalline ZnO films grown at different temperatures. *Chinese Physics B*. 2012. 21(3): 038101-1- 038101-5.
123. Weissler, G. *Methods of experimental physics*. ed. Volume 14. Vacuum Physics and Technology: Academic Press, Inc., New York, NY. 1979.
124. Tsoutsouva, M., C. Panagopoulos and M. Kompitsas. Laser energy density, structure and properties of pulsed-laser deposited zinc oxide films. *Applied Surface Science*. 2011. 257(14): 6314-6319.
125. Sakthivel, S., B. Neppolian, M. Shankar, B. Arabindoo, M. Palanichamy and V. Murugesan. Solar photocatalytic degradation of azo dye: comparison of photocatalytic efficiency of ZnO and TiO₂. *Solar Energy Materials and Solar Cells*. 2003. 77(1): 65-82.
126. Kansal, S., M. Singh and D. Sud. Studies on photodegradation of two commercial dyes in aqueous phase using different photocatalysts. *Journal of hazardous materials*. 2007. 141(3): 581-590.
127. Panthi, G., M. Park, H. Y. Kim, S. Y. Lee and S. J. Park. Electrospun ZnO hybrid nanofibers for photodegradation of wastewater containing organic dyes: a review. *Journal of Industrial and Engineering Chemistry*. 2015. 21: 26-35.
128. Zheng, L., Y. Zheng, C. Chen, Y. Zhan, X. Lin, Q. Zheng, K. Wei and J. Zhu. Network structured SnO₂/ZnO heterojunction nanocatalyst with high photocatalytic activity. *Inorganic Chemistry*. 2009. 48(5): 1819-1825.
129. Marci, G., V. Augugliaro, M. J. Lopez-Munoz, C. Martin, L. Palmisano, V. Rives, M. Schiavello, R. J. Tilley and A. M. Venezia. Preparation characterization and photocatalytic activity of polycrystalline ZnO/TiO₂ systems. 2. Surface, bulk characterization, and 4-nitrophenol photodegradation in liquid-solid regime. *The Journal of Physical Chemistry B*. 2001. 105(5): 1033-1040.

130. Zhang, Z., C. Shao, X. Li, C. Wang, M. Zhang and Y. Liu. Electrospun nanofibers of p-type NiO/n-type ZnO heterojunctions with enhanced photocatalytic activity. *ACS Applied Materials and Interfaces*. 2010. 2(10): 2915-2923.
131. Yu, C., K. Yang, Y. Xie, Q. Fan, C. Y. Jimmy, Q. Shu and C. Wang. Novel hollow Pt-ZnO nanocomposite microspheres with hierarchical structure and enhanced photocatalytic activity and stability. *Nanoscale*. 2013. 5(5): 2142-2151.
132. Grätzel, M. Dye-sensitized solar cells. *Journal of Photochemistry and Photobiology C: Photochemistry Reviews*. 2003. 4(2): 145-153.
133. Fageria, P., S. Gangopadhyay and S. Pande. Synthesis of ZnO/Au and ZnO/Ag nanoparticles and their photocatalytic application using UV and visible light. *RSC Advances*. 2014. 4(48): 24962-24972.
134. Ma, S., R. Li, C. Lv, W. Xu and X. Gou. Facile synthesis of ZnO nanorod arrays and hierarchical nanostructures for photocatalysis and gas sensor applications. *Journal of Hazardous Materials*. 2011. 192(2): 730-740.
135. Yan, H., J. Hou, Z. Fu, B. Yang, P. Yang, K. Liu, M. Wen, Y. Chen, S. Fu and F. Li. Growth and photocatalytic properties of one-dimensional ZnO nanostructures prepared by thermal evaporation. *Materials Research Bulletin*. 2009. 44(10): 1954-1958.
136. Rauf, M. A., M. A. Meetani, A. Khaleel and A. Ahmed. Photocatalytic degradation of methylene blue using a mixed catalyst and product analysis by LC/MS. *Chemical Engineering Journal*. 2010. 157(2): 373-378.
137. Cenens, J. and R. Schoonheydt. Visible spectroscopy of methylene blue on hectorite, laponite B, and barasym in aqueous suspension. *Clays and Clay Minerals*. 1988. 36(3): 214-224.
138. Aguiar, J., B. Bezerra, A. Siqueira, D. Barrera, K. Sapag, D. Azevedo, S. Lucena and I. Silva Jr. Improvement in the adsorption of anionic and cationic dyes from aqueous solutions: A comparative study using aluminium pillared clays and activated carbon. *Separation Science and Technology*. 2014. 49(5): 741-751.
139. Misra, M., P. Kapur, M. K. Nayak and M. Singla. Synthesis and visible photocatalytic activities of a Au@ Ag@ ZnO triple layer core-shell nanostructure. *New Journal of Chemistry*. 2014. 38(9): 4197-4203.

140. Roozbehi, M., P. Sangpour, A. Khademi and A. Z. Moshfegh. The effect of substrate surface roughness on ZnO nanostructures growth. *Applied Surface Science*. 2011. 257(8): 3291-3297.
141. Eichhorn, M. *Laser physics: from principles to practical work in the lab*: Springer Science and Business Media. 2014.
142. Sennaroglu, A. *Solid-state lasers and applications*, ed. Vol. 119: CRC press. 2006.
143. Kim, H. J., J. A. Jeon, J. Y. Choi, J. Kim, J. T. Hong, H. Seo, D. G. Lee, K. J. Lee and M. K. Son. Proposal of optimal process parameters for polymethylmethacryl plastic adhesion using a pulsed Nd: YAG laser. *Optical Engineering*. 2009. 48(8): 084301-084301-7.
144. Makala, R. S., K. Jagannadham and B. C. Sales. Pulsed laser deposition of Bi₂Te₃-based thermoelectric thin films. *Journal of Applied Physics*. 2003. 94(6): 3907-3918.
145. Egerton, R. F. *Physical principles of electron microscopy: an introduction to TEM, SEM, and AEM*: Springer Science and Business Media. 2006.
146. Aneesh, P. *Growth and characterization of nanostructured wide band gap semiconductors for optoelectronic applications*. Thesis Doctor Philosophy. Cochin University of Science and Technology. 2010.
147. Bogner, A., P. H. Jouneau, G. Thollet, D. Basset and C. Gauthier. A history of scanning electron microscopy developments: towards “wet-STEM” imaging. *Micron*. 2007. 38(4): 390-401.
148. Bowen, D. K. and B. K. Tanner. *High resolution X-ray diffractometry and topography*: CRC press. 2005.
149. Hofmann, S. *Auger-and X-ray photoelectron spectroscopy in materials science: a user-oriented guide*, ed. Vol. 49: Springer Science and Business Media. 2012.
150. Gondal, M., Q. Drmosh, Z. Yamani and T. Saleh. Synthesis of ZnO₂ nanoparticles by laser ablation in liquid and their annealing transformation into ZnO nanoparticles. *Applied Surface Science*. 2009. 256(1): 298-304.
151. Tiemann, M., F. Marlow, J. Hartikainen, Ö. Weiss and M. Lindén. Ripening effects in ZnS nanoparticle growth. *The Journal of Physical Chemistry C*. 2008. 112(5): 1463-1467.

152. Sabry, R. and O. AbdulAzeez. Hydrothermal growth of ZnO nano rods without catalysts in a single step. *Manufacturing Letters*. 2014. 2(2): 69-73.
153. Larkin, P. *Infrared and Raman spectroscopy; principles and spectral interpretation*: Elsevier Science. 2011.
154. Adachi, S. *Optical constants of crystalline and amorphous semiconductors: numerical data and graphical information*: Springer Science and Business Media. 1999.
155. Chandrinou, C., N. Boukos, C. Stogios and A. Travlos. PL study of oxygen defect formation in ZnO nanorods. *Microelectronics Journal*. 2009. 40(2): 296-298.
156. Amma, D. S. D., V. Vaidyan and P. Manoj. Structural, electrical and optical studies on chemically deposited tin oxide films from inorganic precursors. *Materials Chemistry and Physics*. 2005. 93(1): 194-201.
157. Moulahi, A. and F. Sediri. ZnO nanoswords and nanopills: Hydrothermal synthesis, characterization and optical properties. *Ceramics International*. 2014. 40(1): 943-950.
158. Ren, C., B. Yang, M. Wu, J. Xu, Z. Fu, T. Guo, Y. Zhao and C. Zhu. Synthesis of Ag/ZnO nanorods array with enhanced photocatalytic performance. *Journal of Hazardous Materials*. 2010. 182(1): 123-129.
159. Wakano, T., N. Fujimura, Y. Morinaga, N. Abe, A. Ashida and T. Ito. Magnetic and magneto-transport properties of ZnO: Ni films. *Physica E: Low-Dimensional Systems and Nanostructures*. 2001. 10(1): 260-264.
160. Cao, B., Z. Liu, H. Xu, H. Gong, D. Nakamura, K. Sakai, M. Higashihata and T. Okada. Catalyst/dopant-free growth of ZnO nanobelts with different optical properties from nanowires grown via a catalyst-assisted method. *CrystEngComm*. 2011. 13(12): 4282-4287.
161. Chee, C. Y., K. Nadarajah, M. K. Siddiqui and Y. Wong. Optical and structural characterization of solution processed zinc oxide nanorods via hydrothermal method. *Ceramics International*. 2014. 40(7): 9997-10004.
162. Tan, S. T., B. Chen, X. Sun, W. Fan, H. Kwok, X. Zhang and S. Chua. Blueshift of optical band gap in ZnO thin films grown by metal-organic chemical-vapor deposition. *Journal of Applied Physics*. 2016. 98: 013505-1-013505-5.

163. Cho, D.-H., J. H. Kim, B. M. Moon, Y. D. Jo and S. M. Koo. Control of a- and c-plane preferential orientations of ZnO thin films. *Applied Surface Science*. 2009. 255(6): 3480-3484.
164. Awad, M., A. Ahmed, V. Khavrus and E. Ibrahim. Tuning the morphology of ZnO nanostructure by in doping and the associated variation in electrical and optical properties. *Ceramics International*. 2015. 41(8): 10116-10124.
165. Rajan, S. T., B. Subramanian, A. N. Kumar, M. Jayachandran and M. R. Rao. Fabrication of nanowires of Al-doped ZnO using nanoparticle assisted pulsed laser deposition (NAPLD) for device applications. *Journal of Alloys and Compounds*. 2014. 584: 611-616.
166. Lyu, S. C., Y. Zhang, H. Ruh, H. J. Lee, H. W. Shim, E. K. Suh and C. J. Lee. Low temperature growth and photoluminescence of well-aligned zinc oxide nanowires. *Chemical Physics Letters*. 2002. 363(1): 134-138.
167. Huang, M. H., Y. Wu, H. Feick, N. Tran, E. Weber and P. Yang. Catalytic growth of zinc oxide nanowires by vapor transport. *Advanced Materials*. 2001. 13(2): 113-116.
168. Hur, T. B., Y. H. Hwang and H. K. Kim. Quantum confinement in Volmer-Weber-type self-assembled ZnO nanocrystals. *Applied Physics Letters*. 2005. 86(19): 193113-1-193113-9.
169. Vinodkumar, R., I. Navas, K. Porsezian, V. Ganesan, N. Unnikrishnan and V. M. Pillai. Structural, spectroscopic and electrical studies of nanostructured porous ZnO thin films prepared by pulsed laser deposition. *Spectrochimica Acta Part A: Molecular and Biomolecular Spectroscopy*. 2014. 118: 724-732.
170. Cao, B., X. Teng, S. H. Heo, Y. Li, S. O. Cho, G. Li and W. Cai. Different ZnO nanostructures fabricated by a seed-layer assisted electrochemical route and their photoluminescence and field emission properties. *The Journal of Physical Chemistry C*. 2007. 111(6): 2470-2476.
171. Van Dijken, A., E. Meulenkaamp, D. Vanmaekelbergh and A. Meijerink. The luminescence of nanocrystalline ZnO particles: the mechanism of the ultraviolet and visible emission. *Journal of Luminescence*. 2000. 87: 454-456.
172. Liu, B. and H. C. Zeng. Direct growth of enclosed ZnO nanotubes. *Nano Research*. 2009. 2(3): 201-209.
173. Lee, Y. J., T. L. Sounart, J. Liu, E. D. Spoecke, B. B. McKenzie, J. W. Hsu and J. A. Voigt. Tunable arrays of ZnO nanorods and nanoneedles via seed

- layer and solution chemistry. *Crystal Growth and Design*. 2008. 8(6): 2036-2040.
174. Ekthammathat, N., S. Thongtem, T. Thongtem and A. Phuruangrat. Characterization and antibacterial activity of nanostructured ZnO thin films synthesized through a hydrothermal method. *Powder Technology*. 2014. 254: 199-205.
175. Gendron-Badou, A. C., T. Coradin, J. Maquet, F. Fröhlich and J. Livage. Spectroscopic characterization of biogenic silica. *Journal of Non-Crystalline Solids*. 2003. 316(2): 331-337.
176. Ivanova, T., A. Harizanova, T. Koutzarova and B. Vertruyen. Study of ZnO sol-gel films: effect of annealing. *Materials Letters*. 2010. 64(10): 1147-1149.
177. Zhai, J., X. Tao, Y. Pu, X. F. Zeng and J. F. Chen. Core/shell structured ZnO/SiO₂ nanoparticles: preparation, characterization and photocatalytic property. *Applied Surface Science*. 2010. 257(2): 393-397.
178. Cun, T., C. Dong and Q. Huang. Ionothermal precipitation of highly dispersive ZnO nanoparticles with improved photocatalytic performance. *Applied Surface Science*. 2016. 384: 73-82.
179. Zak, A. K., M. E. Abrishami, W. A. Majid, R. Yousefi and S. Hosseini. Effects of annealing temperature on some structural and optical properties of ZnO nanoparticles prepared by a modified sol-gel combustion method. *Ceramics International*. 2011. 37(1): 393-398.
180. Suwanboon, S., P. Amornpitoksuk, P. Bangrak and C. Randorn. Physical and chemical properties of multifunctional ZnO nanostructures prepared by precipitation and hydrothermal methods. *Ceramics International*. 2014. 40(1): 975-983.
181. Ko, Y. H. and J. S. Yu. Tunable growth of urchin-shaped ZnO nanostructures on patterned transparent substrates. *CrystEngComm*. 2012. 14(18): 5824-5829.
182. Govender, K., D. S. Boyle, P. B. Kenway and P. O'Brien. Understanding the factors that govern the deposition and morphology of thin films of ZnO from aqueous solution. *Journal of Materials Chemistry*. 2004. 14(16): 2575-2591.
183. Xu, S. and Z. L. Wang. One-dimensional ZnO nanostructures: solution growth and functional properties. *Nano Research*. 2011. 4(11): 1013-1098.

184. Liu, Y., C. Li, J. Wang, X. Fan, G. Yuan, S. Xu, M. Xu, J. Zhang and Y. Zhao. Field emission properties of ZnO nanorod arrays by few seed layers assisted growth. *Applied Surface Science*. 2015. 331: 497-503.
185. Hou, Z., Y. Wang, L. Shen, H. Guo, G. Wang, Y. Li, S. Zhou, Q. Zhang and Q. Jiang. Synthesis of dumbbell-like ZnO microcrystals via a simple solution route. *Nanoscale Research Letters*. 2012. 7(1): 1-7.
186. Ngom, B., T. Mpahane, N. Manyala, O. Nemraoui, U. Buttner, J. Kana, A. Fasasi, M. Maaza and A. Beye. Structural and optical properties of nano-structured tungsten-doped ZnO thin films grown by pulsed laser deposition. *Applied Surface Science*. 2009. 255(7): 4153-4158.
187. Zhao, J., L. Hu, Z. Wang, J. Sun and Z. Wang. ZnO thin films on Si (111) grown by pulsed laser deposition from metallic Zn target. *Applied Surface Science*. 2006. 253(2): 841-845.
188. Ramakrishna, G. and H. N. Ghosh. Effect of particle size on the reactivity of quantum size ZnO nanoparticles and charge-transfer dynamics with adsorbed catechols. *Langmuir*. 2003. 19(7): 3006-3012.
189. Li, Q., V. Kumar, Y. Li, H. Zhang, T. J. Marks and R. P. Chang. Fabrication of ZnO nanorods and nanotubes in aqueous solutions. *Chemistry of Materials*. 2005. 17(5): 1001-1006.
190. Qu, J., C. Y. Cao, Y. L. Hong, C. Q. Chen, P. P. Zhu, W. G. Song and Z. Y. Wu. New hierarchical zinc silicate nanostructures and their application in lead ion adsorption. *Journal of Materials Chemistry*. 2012. 22(8): 3562-3567.
191. Xu, H., C. Wei, C. Li, G. Fan, Z. Deng, M. Li and X. Li. Sulfuric acid leaching of zinc silicate ore under pressure. *Hydrometallurgy*. 2010. 105(1): 186-190.
192. Zamiri, R., A. Rebelo, G. Zamiri, A. Adnani, A. Kuashal, M. S. Belsley and J. Ferreira. Far-infrared optical constants of ZnO and ZnO/Ag nanostructures. *RSC Advances*. 2014. 4(40): 20902-20908.
193. Pholnak, C., C. Sirisathitkul, S. Suwanboon and D. J. Harding. Effects of precursor concentration and reaction time on sonochemically synthesized ZnO nanoparticles. *Materials Research*. 2014. 17(2): 405-411.
194. Stuart, B. *Infrared spectroscopy*: Wiley and Sons, Inc., 2005.
195. Trezza, M. A. Hydration study of ordinary Portland cement in the presence of zinc ions. *Materials Research*. 2007. 10(4): 331-334.

196. Latthe, S. S., S. Liu, C. Terashima, K. Nakata and A. Fujishima. Transparent, Adherent, and Photocatalytic SiO₂-TiO₂ Coatings on Polycarbonate for Self-Cleaning Applications. *Coatings*. 2014. 4(3): 497-507.
197. Wang, Y., J. Yang, H. Jia, M. Yu and H. Jin. Self-assembled urchin-like ZnO nanostructures fabricated by electrodeposition-hydrothermal method. *Journal of Alloys and Compounds*. 2016. 665: 62-68.
198. Mahmood, K., S. B. Park and H. J. Sung. Enhanced photoluminescence, Raman spectra and field-emission behavior of indium-doped ZnO nanostructures. *Journal of Materials Chemistry C*. 2013. 1(18): 3138-3149.
199. Zhao, C., A. Chen, X. Ji, Y. Zhu, X. Gui, F. Huang and Z. Tang. Growth of vertically aligned ZnO nanowire arrays on ZnO single crystals. *Materials Letters*. 2015. 154: 40-43.
200. Liqiang, J., Q. Yichun, W. Baiqi, L. Shudan, J. Baojiang, Y. Libin, F. Wei, F. Honggang and S. Jiazhong. Review of photoluminescence performance of nano-sized semiconductor materials and its relationships with photocatalytic activity. *Solar Energy Materials and Solar Cells*. 2006. 90(12): 1773-1787.
201. Panigrahy, B., M. Aslam, D. S. Misra, M. Ghosh and D. Bahadur. Defect-related emissions and magnetization properties of ZnO nanorods. *Advanced Functional Materials*. 2010. 20(7): 1161-1165.
202. Sugunan, A., H. C. Warad, M. Boman and J. Dutta. Zinc oxide nanowires in chemical bath on seeded substrates: role of hexamine. *Journal of Sol-Gel Science and Technology*. 2006. 39(1): 49-56.
203. Usui, H., Y. Shimizu, T. Sasaki and N. Koshizaki. Photoluminescence of ZnO nanoparticles prepared by laser ablation in different surfactant solutions. *The Journal of Physical Chemistry B*. 2005. 109(1): 120-124.
204. Zhang, C. and J. Lin. Defect-related luminescent materials: synthesis, emission properties and applications. *Chemical Society Reviews*. 2012. 41(23): 7938-7961.
205. Rashid, T. R., D. T. Phan and G. S. Chung. A flexible hydrogen sensor based on Pd nanoparticles decorated ZnO nanorods grown on polyimide tape. *Sensors and Actuators B: Chemical*. 2013. 185: 777-784.
206. Ahn, M. W., K. S. Park, J. H. Heo, J. G. Park, D. W. Kim, K. J. Choi, J. H. Lee and S. H. Hong. Gas sensing properties of defect-controlled ZnO-

- nanowire gas sensor. *Applied Physics Letters*. 2008. 93(26): 263103-1-263103-3.
207. Yang, C., Q. Li, L. Tang, K. Xin, A. Bai and Y. Yu. Synthesis, photocatalytic activity, and photogenerated hydroxyl radicals of monodisperse colloidal ZnO nanospheres. *Applied Surface Science*. 2015. 357: 1928-1938.
208. Srivastava, V., D. Gusain and Y. C. Sharma. Synthesis, characterization and application of zinc oxide nanoparticles (n-ZnO). *Ceramics International*. 2013. 39(8): 9803-9808.
209. Lin, K. F., H. M. Cheng, H. C. Hsu, L. J. Lin and W. F. Hsieh. Band gap variation of size-controlled ZnO quantum dots synthesized by sol-gel method. *Chemical Physics Letters*. 2005. 409(4): 208-211.
210. Zhang, T., Y. Zeng, H. Fan, L. Wang, R. Wang, W. Fu and H. Yang. Synthesis, optical and gas sensitive properties of large-scale aggregative flowerlike ZnO nanostructures via simple route hydrothermal process. *Journal of Physics D: Applied Physics*. 2009. 42(4): 045103-1-045103-8.
211. Zhang, C., M. Shao, F. Ning, S. Xu, Z. Li, M. Wei, D. G. Evans and X. Duan. Au nanoparticles sensitized ZnO nanorod@ nanoplatelet core-shell arrays for enhanced photoelectrochemical water splitting. *Nano Energy*. 2015. 12: 231-239.
212. Chang, Y. M., P. H. Kao, M. C. Liu, C. M. Lin, H. Y. Lee and J. Y. Juang. Fabrication and optoelectronic properties of core-shell biomimetic ZnO/Si nanoball arrays. *RSC Advances*. 2012. 2(29): 11089-11094.
213. Liu, T., Y. Li, H. Zhang, M. Wang, X. Fei, S. Duo, Y. Chen, J. Pan and W. Wang. Tartaric acid assisted hydrothermal synthesis of different flower-like ZnO hierarchical architectures with tunable optical and oxygen vacancy-induced photocatalytic properties. *Applied Surface Science*. 2015. 357: 516-529.
214. Jitianu, M. and D. V. Goia. Zinc oxide colloids with controlled size, shape, and structure. *Journal of Colloid and Interface Science*. 2007. 309(1): 78-85.
215. Al-Asedy, H. J., A. M. Al-Azawi, N. Bidin and K. N. Abbs. ZnO QDs Deposited on Si by Sol-Gel Method: Role of Annealing Temperature on Structural and Optical Properties. *Modern Applied Science*. 2016. 10(4): 12-20.

216. Degen, A. and M. Kosec. Effect of pH and impurities on the surface charge of zinc oxide in aqueous solution. *Journal of the European Ceramic Society*. 2000. 20(6): 667-673.
217. Cross, R., M. De Souza and E. S. Narayanan. A low temperature combination method for the production of ZnO nanowires. *Nanotechnology*. 2005. 16(10): 2188-20192.
218. Dong, B., X. Yu, Z. Dong, X. Yang and Y. Wu. Facile synthesis of ZnO nanoparticles for the photocatalytic degradation of methylene blue. *Journal of Sol-Gel Science and Technology*. 2016: 1-10.
219. Mimouni, R., A. Souissi, A. Madouri, K. Boubaker and M. Amlouk. High photocatalytic efficiency and stability of chromium-indium codoped ZnO thin films under sunlight irradiation for water purification development purposes. *Current Applied Physics*. 2017. 17(8): 1058-1065.
220. Singh, J., K. Sahu, S. Kuriakose, N. Tripathi, D. Avasthi and S. Mohapatra. Synthesis of nanostructured TiO₂ thin films with highly enhanced photocatalytic activity by atom beam sputtering. *Advanced Materials Letters*. 2017. 8: 107-113.
221. Bensouici, F., M. Bououdina, A. Dakhel, R. Tala-Ighil, M. Tounane, A. Iratni, T. Souier, S. Liu and W. Cai. Optical, structural and photocatalysis properties of Cu-doped TiO₂ thin films. *Applied Surface Science*. 2017. 395: 110-116.
222. Pongchan, G., B. Ksapabutr and M. Panapoy. One-step synthesis of flower-like carbon-doped ZrO₂ for visible-light-responsive photocatalyst. *Materials and Design*. 2016. 89: 137-145.
223. Helal, A., F. A. Harraz, A. A. Ismail, T. M. Sami and I. Ibrahim. Hydrothermal synthesis of novel heterostructured Fe₂O₃/Bi₂S₃ nanorods with enhanced photocatalytic activity under visible light. *Applied Catalysis B: Environmental*. 2017. 213: 18-27.
224. Chandran, D., L. S. Nair, S. Balachandran, K. R. Babu and M. Deepa. Band gap narrowing and photocatalytic studies of Nd³⁺ ion-doped SnO₂ nanoparticles using solar energy. *Bulletin of Materials Science*. 2016. 39(1): 27-33.
225. Abbas, N., G. N. Shao, S. M. Imran, M. S. Haider and H. T. Kim. Inexpensive synthesis of a high-performance Fe₃O₄-SiO₂-TiO₂ photocatalyst:

- Magnetic recovery and reuse. *Frontiers of Chemical Science and Engineering*. 2016. 10(3): 405-416.
226. Peng, Z. and H. Yang. Designer platinum nanoparticles: Control of shape, composition in alloy, nanostructure and electrocatalytic property. *Nano Today*. 2009. 4(2): 143-164.
227. Samavati, A., Z. Othaman, S. Ghoshal and M. Mustafa. Effects of annealing temperature on shape transformation and optical properties of germanium quantum dots. *Chinese Physics B*. 2015. 24(2): 028103-1-028103-6.
228. Du, J., R. Zhao and Y. Xue. Effects of sizes of nano-copper oxide on the equilibrium constant and thermodynamic properties for the reaction in nanosystem. *The Journal of Chemical Thermodynamics*. 2012. 45(1): 48-52.
229. Sheela, T., Y. A. Nayaka, R. Viswanatha, S. Basavanna and T. Venkatesha. Kinetics and thermodynamics studies on the adsorption of Zn (II), Cd (II) and Hg (II) from aqueous solution using zinc oxide nanoparticles. *Powder Technology*. 2012. 217: 163-170.